

BRIDGE TRISECTIONS IN \mathbb{CP}^2 AND THE THOM CONJECTURE

PETER LAMBERT-COLE

ABSTRACT. In this paper, we develop new techniques for understanding surfaces in \mathbb{CP}^2 via bridge trisections. Trisections are a novel approach to smooth 4-manifold topology, introduced by Gay and Kirby, that provide an avenue to apply 3-dimensional tools to 4-dimensional problems. Meier and Zupan subsequently developed the theory of bridge trisections for smoothly embedded surfaces in 4-manifolds. The main application of these techniques is a new proof of the Thom conjecture, which posits that algebraic curves in \mathbb{CP}^2 have minimal genus among all smoothly embedded, oriented surfaces in their homology class. This new proof is notable as it completely avoids any gauge theory or pseudoholomorphic curve techniques.

1. INTRODUCTION

A trisection of a smooth, oriented 4-manifold X is a particular decomposition into three elementary pieces. It is a 4-dimensional analogue of Heegaard splittings, where a 3-manifold is bisected into two handlebodies glued together along their boundary. Recently, Meier and Zupan have extended this perspective to bridge trisections of knotted surfaces in 4-manifolds [MZ17b, MZ17a]. Bridge trisections are a 4-dimensional analogue of bridge position for links in a 3-manifold. A bridge splitting of a link L is a decomposition of L into a pair of trivial tangles. Similarly, a bridge trisection of a knotted surface is a decomposition into a triple of trivial disk tangles.

The projective plane \mathbb{CP}^2 admits a genus 1 trisection well-adapted to its complex and toric geometry. This geometric compatibility makes it possible to apply topological methods in 3-dimensional contact geometry to the study of smooth surfaces in \mathbb{CP}^2 . In this paper, we introduce several new techniques, concepts and results regarding bridge trisections and diagrams for bridge trisections. The main application is a new proof of the Thom conjecture.

Theorem 1.1 (Thom Conjecture [KM94]). *Let \mathcal{K} be a smoothly embedded, oriented, connected surface in \mathbb{CP}^2 of degree $d > 0$. Then*

$$g(\mathcal{K}) \geq \frac{1}{2}(d-1)(d-2).$$

The conjecture was originally proved by Kronheimer and Mrowka using Seiberg-Witten gauge theory [KM94]. A generalization to Kahler manifolds, that complex curves minimize genus, was subsequently proved by Morgan, Szabo and Taubes [MST96]. Alternate proofs of the original conjecture in \mathbb{CP}^2 were subsequently given by Ozsvath and Szabo using Heegaard-Floer homology [OS03] and by Strle [Str03].

The novelty of this trisections proof is that we completely avoid any gauge theory or pseudoholomorphic curve techniques. In particular, using the techniques introduced in this paper, we can reduce the adjunction inequality to the *ribbon-Bennequin inequality*.

2010 *Mathematics Subject Classification.* 57R17, 57R40.

Key words and phrases. Thom conjecture, 4-manifolds, bridge trisections, minimal genus.

Theorem 1.2 (Ribbon-Bennequin inequality). *Let L be a transverse link in (S^3, ξ_{std}) and let F be a ribbon surface bounded by L . Then*

$$sl(L) \leq -\chi(F).$$

This is the ribbon surface equivalent of the well-known *slice-Bennequin inequality*, which was conjectured by Bennequin [Ben83] and first proved by Rudolph [Rud93]. Rudolph proved that slice-Bennequin is equivalent to the *Local Thom conjecture* on the slice genera of torus knots.

Theorem 1.3 (Local Thom Conjecture [KM93]). *The slice genus of $T(p, q)$ is $\frac{1}{2}(p-1)(q-1)$.*

The Local Thom conjecture was also proved by Kronheimer and Mrowka [KM93], using Donaldson invariants. Later, Rasmussen [Ras10] introduced a concordance invariant in Khovanov homology and reestablished the slice genera of torus knots. Shumakovitch [Shu07] then noted that the slice-Bennequin inequality is an easy consequence. Consequently, as the slice-Bennequin inequality trivially implies the ribbon-Bennequin inequality, our proof of Theorem 1.1 reduces to Rasmussen's combinatorial proof and avoids gauge theory.

In effect, the proof uses the Local Thom conjecture to deduce the (global) Thom conjecture. This reverses the standard approach, such as in [KM94, LM98], whereby a global adjunction inequality is used to deduce information about slice genera. As the Local Thom conjecture can be easily deduced from the global version, we have the following corollary.

Theorem 1.4. *The Thom conjecture is equivalent to the Local Thom conjecture.*

Moreover, based on the way in which a trisection decomposition shuffles the topology of a 4-manifold, it seems plausible to apply this strategy and recover adjunction inequalities in larger 4-manifolds. For example, the most general version of Theorem 1.1 is the *symplectic Thom conjecture*, proved by Ozsvath and Szabo [OS00b], which posits that symplectic surfaces in a symplectic 4-manifold minimize genus in their homology class. There has been some progress in trisections of Kahler surfaces and curves on them [MZ17a, LM18]. However, the interaction between trisections and Kahler or symplectic geometry remains a deep open question.

Finally, as mentioned above, our proof reduces to the ribbon-Bennequin inequality. Interestingly, this is purely a 3-dimensional statement, as opposed to the 4-dimensional slice-Bennequin inequality. It would be extremely interesting to give a proof using only 3-dimensional contact geometry, perhaps by reducing it to the Bennequin-Eliashberg inequality. Given the deep geometric connection between tight contact structures and the adjunction inequality, this would complete an extremely satisfying proof of the Thom conjecture.

1.1. Trisections. Let X be a smooth, closed, oriented 4-manifold. A $(d+1)$ -dimensional *1-handlebody* of genus g is the compact $(d+1)$ -manifold $\natural^g(S^1 \times D^d)$.

Definition 1.5 ([GK16]). A $(g; k_1, k_2, k_3)$ -trisection \mathcal{T} of X is a decomposition $X = X_1 \cup X_2 \cup X_3$ such that

- (1) Each X_λ is a 4-dimensional 1-handlebody of genus k_i ,
- (2) Each $H_\lambda = X_{\lambda-1} \cap X_\lambda$ is a 3-dimensional 1-handlebody of genus g , and
- (3) $\Sigma = X_1 \cap X_2 \cap X_3$ is a closed, oriented surface of genus g

If $k_1 = k_2 = k_3 = k$, we call \mathcal{T} a (g, k) -trisection of X .

The orientation of X induces orientations on each X_λ and each boundary $Y_\lambda := \partial X_\lambda$. We choose to orient H_λ by viewing it as a submanifold of Y_λ . As a result, the orientation induced on Σ as the boundary of H_λ is independent of λ . Moreover, we have that $Y_\lambda = H_\lambda \cup_\Sigma -H_{\lambda+1}$ as oriented manifolds.

The *spine* of a trisection \mathcal{T} is the union $H_1 \cup H_2 \cup H_3$. The spine uniquely determines the trisection \mathcal{T} and can be encoded by a *trisection diagram* (α, β, γ) consisting of three cut systems for Σ . A cut system for Σ consists of g disjoint, simple closed curves whose complement in Σ is a planar surface. Each cut system corresponds to one handlebody H_λ . The spine is constructed by attaching 2-handles along each curve in the cut system, followed by a single 3-handle for each handlebody H_λ . If X admits a $(g; k_1, k_2, k_3)$ trisection, then

$$\chi(X) = 2 + g - k_1 - k_2 - k_3.$$

1.2. Trisection of \mathbb{CP}^2 . The toric geometry of \mathbb{CP}^2 yields a trisection \mathcal{T} as follows. Define the moment map $\mu : \mathbb{CP}^2 \rightarrow \mathbb{R}^2$ by the formula

$$\mu([z_1 : z_2 : z_3]) := \left(\frac{3|z_1|}{|z_1| + |z_2| + |z_3|}, \frac{3|z_2|}{|z_1| + |z_2| + |z_3|} \right).$$

The image of μ is the convex hull of the points $\{(0, 0), (3, 0), (0, 3)\}$. The fiber of μ over an interior point is T^2 ; the fibers over an interior point of a face of the polytope is S^1 ; and the fiber over a vertex is a point. The preimage of an entire face of the polytope is a complex line $L_\lambda = \{[z_1 : z_2 : z_3] : z_\lambda = 0\}$ for some λ .

The barycentric subdivision of the simplex $\mu(\mathbb{CP}^2)$ lifts to a trisection decomposition of \mathbb{CP}^2 . Define subsets

$$\begin{aligned} X_\lambda &:= \{[z_1 : z_2 : z_3] : |z_\lambda|, |z_{\lambda+1}| \leq |z_{\lambda-1}|\}, \\ H_\lambda &:= \{[z_1 : z_2 : z_3] : |z_\lambda| \leq |z_{\lambda-1}| = |z_{\lambda+1}|\}. \end{aligned}$$

In the affine chart on \mathbb{CP}^2 obtained by setting $z_3 = 1$, the handlebody X_1 is exactly the polydisk

$$\Delta = \mathbb{D} \times \mathbb{D} = \{(z_1, z_2) : |z_1|, |z_2| \leq 1\}.$$

Its boundary is the union of two solid tori

$$H_1 = S^1 \times \mathbb{D} \quad \text{and} \quad H_2 = \mathbb{D} \times S^1.$$

The triple intersection $X_1 \cap X_2 \cap X_3$ is the torus

$$\Sigma := \{[e^{i\theta_1} : e^{i\theta_2} : 1] : \theta_1, \theta_2 \in [0, 2\pi]\}.$$

Furthermore, the intersection $B_\lambda = L_\lambda \cap H_\lambda$ is a core circle of the solid torus.

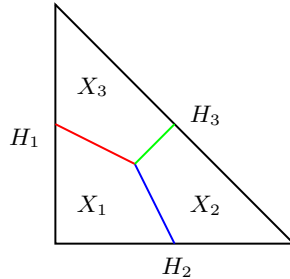


FIGURE 1. The moment polytope of \mathbb{CP}^2 , with the trisection decomposition described.

We therefore have shown the following proposition.

Proposition 1.6. *The decomposition $\mathbb{CP}^2 = X_1 \cup X_2 \cup X_3$ is a $(1, 0)$ trisection.*

1.3. Bridge trisections. Let $\{\tau_i\}$ be a collection of properly embedded arcs in a handlebody H . An arc collection is *trivial* if they can be simultaneously isotoped to lie in ∂H . If $\{\tau_i\}$ is trivial, then there exist a collection of disjoint disks $\Delta = \{\Delta_i\}$, embedded in H , such that $\partial\Delta_i = \tau_i \cup s_i$ where s_i is an arc in $\partial\Sigma$. We call each Δ_i a *bridge disk* and the arc s_i the *shadow* of τ_i . A *bridge splitting* of a link L is the 3-manifold Y is a decomposition $(Y, L) = (H_1, \tau_1) \cup_\Sigma (H_2, \tau_2)$ where H_1, H_2 are handlebodies and the arc collections τ_1, τ_2 are trivial. Finally, a collection $\mathcal{D} = \{\mathcal{D}_i\}$ of properly embedded disks in a 1-handlebody X are *trivial* if they can be simultaneously isotoped to lie in ∂X .

Definition 1.7. A $(b; c_1, c_2, c_3)$ *bridge trisection* of a knotted surface (X, \mathcal{K}) is a decomposition $(X, \mathcal{K}) = (X_1, \mathcal{D}_1) \cup (X_2, \mathcal{D}_2) \cup (X_3, \mathcal{D}_3)$ such that

- (1) $X = X_1 \cup X_2 \cup X_3$ is a trisection of X ,
- (2) each \mathcal{D}_λ is a collection of c_λ trivial disks in X_λ , and
- (3) each tangle $\tau_\lambda = \mathcal{D}_{\lambda-1} \cap \mathcal{D}_\lambda$, for $i \neq j$, is trivial.

If (X, \mathcal{K}) admits a bridge trisection, we say that \mathcal{K} is in *bridge position*.

Let $K_\lambda \subset Y_\lambda$ be the boundary of the trivial disk system \mathcal{D}_λ . Since \mathcal{D}_λ is trivial, the link K_λ is the unlink with c_λ components. If \mathcal{K} is oriented, then each trivial disk system \mathcal{D}_λ inherits this orientation. We choose to orient τ_λ by viewing it as a submanifold of $\partial\mathcal{D}_\lambda$. With these conventions, the induced orientation on the points of $\partial\tau_\lambda$ is independent of λ and moreover agrees with their induced orientation as the transverse intersection $\Sigma \pitchfork \mathcal{K}$. Finally, we have $(Y_\lambda, K_\lambda) = (H_\lambda, \tau_\lambda) \cup_\Sigma (-H_{\lambda+1}, \tau_{\lambda+1}^r)$ as oriented manifolds.

The main result of [MZ17a] is that every knotted smooth surface (X, \mathcal{K}) can be put into bridge position.

Theorem 1.8 ([MZ17a]). *Let \mathcal{T} be a trisection of a closed, connected, oriented smooth 4-manifold X . Every smoothly embedded surface \mathcal{K} in X can be isotoped into bridge position with respect to \mathcal{T} .*

The *spine* of a surface \mathcal{K} in bridge position is the union $\tau_1 \cup \tau_2 \cup \tau_3$. The spine uniquely determines the generalized bridge trisection of \mathcal{K} [MZ17a, Corollary 2.4]. If \mathcal{K} admits a $(b; c_1, c_2, c_3)$ bridge trisection, then

$$(1) \quad \chi(\mathcal{K}) = c_1 + c_2 + c_3 - b.$$

1.4. Transverse bridge position. In Section 3, we introduce *transverse bridge position* and *transverse torus diagrams*. The motivation was to find a class of bridge trisections and diagrams that have geometric rigidity, in analogy to grid diagrams for knots in S^3 . However, initial attempts suggest that it is unlikely for there to be a suitable notion of grid diagrams for surfaces in \mathbb{CP}^2 .

In homogeneous coordinates, the handlebody H_λ can equivalently be defined as

$$H_\lambda := \{[z_1 : z_2 : z_3] : |z_\lambda| \leq 1, |z_{\lambda+1}| = 1, z_{\lambda-1} = 1\}$$

Using standard polar coordinates

$$z_\lambda = r_\lambda e^{i\theta_\lambda} \quad z_{\lambda+1} = r_{\lambda+1} e^{i\theta_{\lambda+1}}$$

we have coordinates $(\theta_{\lambda+1}, r_\lambda, \theta_\lambda)$ on $H_\lambda = S^1 \times \mathbb{D}$. The solid torus H_λ is foliated by holomorphic disks. The plane field tangent to this foliation is the kernel of the 1-form $d\theta_{\lambda+1}$.

The complex geometry of \mathbb{CP}^2 naturally induces contact structures on each 3-manifold Y_λ of the trisection decomposition. Specifically, each piece X_λ of the trisection decomposition can be approximated by a Stein domain $\widehat{X}_{\lambda,N}$ in its interior and the hyperplane field $\widehat{\xi}_{\lambda,N}$ of complex tangencies on its boundary $\widehat{Y}_{\lambda,N} \cong S^3$ is the standard tight contact structure. As $\widehat{X}_{\lambda,N}$ converges to X_λ , the contact structure $\widehat{\xi}_{\lambda,N}$ converges nonuniformly to the foliations of $H_\lambda, -H_{\lambda+1}$ by holomorphic disks.

A knotted surface $(\mathbb{CP}^2, \mathcal{K})$ in \mathbb{CP}^2 in general position with respect to the standard genus 1 trisection is *geometrically transverse* if, in each solid torus H_λ , the arcs of the spine are positively transverse to the foliation by holomorphic disks. If $(\mathbb{CP}^2, \mathcal{K})$ is in bridge position and is geometrically transverse, we say that it is in *transverse bridge position*. If a surface is geometrically transverse, then for N sufficiently large it intersects each $(\widehat{Y}_{N,\lambda}, \widehat{\xi}_{\lambda,N})$ along a transverse link. Furthermore, if it is in transverse bridge position then it intersects along transverse unlinks.

Every surface in transverse bridge position satisfies the adjunction inequality. The degree, self-intersection number and Euler characteristic of \mathcal{K} , along with the self-linking numbers of the transverse links in each \widehat{Y}_i , can be easily computed from a torus diagram. Combining these with the Bennequin bound on the self-linking number yields the required bound.

Theorem 1.9. *Let $(\mathbb{CP}^2, \mathcal{K})$ be a connected, oriented surface of degree d in transverse bridge position. Then \mathcal{K} satisfies the adjunction inequality:*

$$\chi(\mathcal{K}) \leq 3d - d^2.$$

An immediate corollary is that there are surfaces in \mathbb{CP}^2 that cannot be put into transverse bridge position. For example, nullhomologous spheres violate the adjunction inequality. A natural question is therefore:

Question 1.10. *Which surfaces can be isotoped into transverse bridge position?*

It is unknown whether every essential surface in \mathbb{CP}^2 can be put into transverse bridge position. All complex curves in \mathbb{CP}^2 can be isotoped into transverse bridge position [LM18]. But the class of surfaces admitting transverse bridge presentations includes more than just complex curves and symplectic surfaces. It is straightforward to attach handles and obtain surfaces in transverse bridge position with nonminimal genus, which therefore cannot be symplectic.

1.5. Algebraic transversality and adjunction. As mentioned above, there are surfaces in \mathbb{CP}^2 that cannot be isotoped into transverse bridge position. To prove Theorem 1.1 in full generality, we introduce the weaker notion of *algebraic transverse bridge position*.

Recall that the solid torus $H_\lambda \cong S^1 \times \mathbb{D}$ is foliated by holomorphic disks. In polar coordinates on H_λ , the plane field tangent to the foliation is the kernel of the 1-form $d\theta_{\lambda+1}$. A knotted surface $(\mathbb{CP}^2, \mathcal{K})$ in \mathbb{CP}^2 is *algebraically transverse* if for each λ , the integral of $d\theta_{\lambda+1}$ along each component of τ_λ is positive. Clearly, a surface in transverse bridge position is also in algebraic transverse bridge position. In addition, this geometric condition is sufficiently flexible to accomodate every surface of positive degree.

Theorem 1.11. *Let $(\mathbb{CP}^2, \mathcal{K})$ be a connected, oriented surface of degree $d > 0$. Then \mathcal{K} can be isotoped into algebraic transverse bridge position.*

By further manipulations, we can completely isolate the obstruction to isotoping an algebraically transverse surface to be geometrically transverse. Specifically, we can reduce to the case where the bridge trisection of a surface \mathcal{K} has a finite number of simple clasps (see Figure 11). These clasps may be undone by a regular homotopy of the spine of the bridge trisection, which corresponds to a finger

move of the surface \mathcal{K} . The result is an immersed but geometrically transverse surface that intersects each \hat{Y}_i along a transverse link. Applying the ribbon-Bennequin inequality to a modification of this link, we can recover the adjunction inequality and prove Theorem 1.1.

Theorem 1.12. *Let $(\mathbb{CP}^2, \mathcal{K})$ be a connected, oriented surface of degree d in algebraic transverse bridge position. Then \mathcal{K} satisfies the adjunction inequality.*

$$\chi(\mathcal{K}) \leq 3d - d^2.$$

1.6. Acknowledgements. I am deeply indebted to my long-term conversation partners, John Etnyre and Jeff Meier. In addition, I would like to thank David Gay, Tye Lidman, Chuck Livingston, Gordana Matic, Paul Melvin and Alex Zupan for helpful comments and encouragement.

2. DIAGRAMS FOR SURFACES IN \mathbb{CP}^2

Given a surface $(\mathbb{CP}^2, \mathcal{K})$ in general position with respect to the standard trisection, we can obtain a *torus diagram* $\mathcal{S}(\mathcal{K}) = (\mathcal{A}, \mathcal{B}, \mathcal{C})$ on the central surface Σ of the trisection. Algebraic information about \mathcal{K} , including its homology class and normal Euler number, can be computed from the diagram $\mathcal{S}(\mathcal{K})$.

2.1. Trisection Diagram for \mathbb{CP}^2 . To obtain a trisection diagram for the standard trisection of \mathbb{CP}^2 , first note that the handlebody H_1 is foliated by the holomorphic disks $\{[e^{i\theta_1} : 1 : 1]\} \times \mathbb{D}$. Thus the curve $\alpha := \{[e^{i\theta_1} : 1 : 1]\}$ bounds a disk in H_1 . Similarly, the curves $\beta := \{[1 : e^{i\theta_2} : 1]\}$ and $\gamma := \{[1 : 1 : e^{i\theta_3}]\}$ bound disks in H_2 and H_3 , respectively. Therefore, the triple $\{\alpha, \beta, \gamma\}$ is a trisection diagram for this trisection of \mathbb{CP}^2 . We will also use the notation

$$\alpha_1 := \alpha \quad \alpha_2 := \beta \quad \alpha_3 := \gamma$$

when appropriate.

2.2. Handlebody coordinates. The natural coordinates on \mathbb{CP}^2 are homogeneous, not absolute. Many of the arguments, definitions and statements are triply-symmetric and it is convenient to work in different affine charts on \mathbb{CP}^2 . We adopt the following convention. When describing an object associated to a fixed but unspecified $\lambda \in \{1, 2, 3\}$ — such as $H_\lambda, Y_\lambda, \tau_\lambda$, etc... — we will use the coordinates inherited from the affine chart $z_{\lambda-1} = 1$.

For example, when $\lambda = 2$, we set $z_1 = 1$ in homogeneous coordinates and obtain affine coordinates z_2, z_3 . In polar form, we then have

$$z_2 = r_2 e^{i\theta_2} \quad z_3 = r_3 e^{i\theta_3}$$

These restrict to give coordinates $(\theta_3, r_2, \theta_2)$ on $H_2 \cong S^1 \times \mathbb{D}$. However, the solid torus H_2 (with the opposite orientation) is also contained in Y_1 . It has a second coordinate system, denoted by $(\theta_1, r_2, \theta_2)$, that is induced by setting $z_3 = 1$. Beware that despite equivalent notation, the angular coordinate θ_2 differs between the two systems and depends on context (whether $\lambda = 1$ or $\lambda = 2$).

2.3. Orientations. The standard orientation on \mathbb{CP}^2 orients each of the pieces of the trisection as follows. Let Y_λ be oriented as the boundary of X_λ , with outward-normal-first convention. In particular, in the affine chart obtained by setting $z_{\lambda-1} = 1$, we have coordinates

$$z_\lambda = r_\lambda e^{i\theta_\lambda} \quad z_{\lambda+1} = r_{\lambda+1} e^{i\theta_{\lambda+1}}$$

and a frame $\{\partial_{r_\lambda}, \partial_{\theta_\lambda}, \partial_{r_{\lambda+1}}, \partial_{\theta_{\lambda+1}}\}$ for TX_λ . Along H_λ , the vector $\partial_{r_{\lambda+1}}$ is the outward normal to X_λ , so the frame $\{\partial_{\theta_{\lambda+1}}, \partial_{r_\lambda}, \partial_{\theta_\lambda}\}$ determines the orientation on Y_λ . We fix an orientation $H_\lambda \subset Y_\lambda$ by restriction. Finally, we orient the central surface Σ as the boundary of $H_\lambda \subset Y_\lambda$, with its

induced orientation. Since ∂_{r_λ} is the outward normal, we get an oriented frame $\{\partial_{\theta_\lambda}, \partial_{\theta_{\lambda+1}}\}$ on Σ . As the construction is triply-symmetric, the induced orientation on the central surface Σ is well-defined independent of $\lambda \in \{1, 2, 3\}$.

The canonical orientation of the holomorphic disks induces an orientation on each curve α, β, γ . In homology, we have that

$$[\gamma] = -[\alpha] - [\beta].$$

Furthermore, each pair

$$\{[\alpha], [\beta]\} \quad \{[\beta], [\gamma]\} \quad \{[\gamma], [\alpha]\}$$

is an oriented basis for $H_1(\Sigma; \mathbb{Z})$.

2.4. Surfaces in \mathbb{CP}^2 . Let $(\mathbb{CP}^2, \mathcal{K})$ be an immersed surface. After a perturbation, we can assume that \mathcal{K} is in general position with respect to the genus-1 trisection of \mathbb{CP}^2 . Specifically, the surface \mathcal{K} intersects the central surface Σ transversely in $2b$ points; that \mathcal{K} intersects each solid torus H_λ transversely along a tangle τ_λ ; and that all of the self-intersections of \mathcal{K} are disjoint from the spine of the trisection. By abuse of terminology, we refer to the points of $\mathcal{K} \cap \Sigma$ as the *bridge points* of \mathcal{K} and b as the *bridge index* of \mathcal{K} . Moreover, after a perturbation we can assume that each tangle τ_λ is disjoint from the core B_λ of H_λ .

Recall that we have chosen orientations on each handlebody H_λ and the central surface Σ is oriented. If \mathcal{K} is oriented, we get orientations on the $2b$ points of $\mathcal{K} \cap \Sigma$ and the b arcs of $\tau_\lambda = \mathcal{K} \cap H_\lambda$. For a bridge point v , let $\sigma(v)$ denote this orientation. Since Σ is nullhomologous, the algebraic intersection number $[\mathcal{K}] \cdot [\Sigma]$ vanishes and so we exactly b positive bridge points and b negative bridge points. The orientation on a bridge point agrees with its orientation as the boundary of every tangle arc. In particular, if the oriented boundary of some arc $\tau_{\lambda,i}$ is $v_1 - v_2$, then $\sigma(v_1) = 1$ and $\sigma(v_2) = -1$.

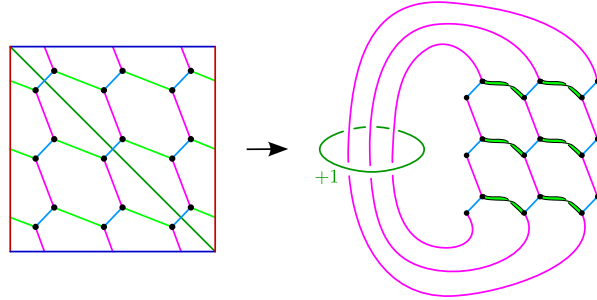


FIGURE 2. (Left) A torus diagram for the $(1,0;9,3)$ bridge trisection of a cubic curve in \mathbb{CP}^2 . (Right) A banded link diagram corresponding to the bridge splitting of the cubic.

2.5. Torus diagrams of surfaces in \mathbb{CP}^2 . Define the projection map $\pi_\lambda : H_\lambda \setminus B_\lambda \rightarrow \Sigma$ in coordinates by

$$\pi_\lambda(\theta_{\lambda+1}, r_\lambda, \theta_\lambda) := (\theta_\lambda, \theta_{\lambda+1})$$

Let $(\mathbb{CP}^2, \mathcal{K})$ be an immersed surface in general position. Set $\mathcal{A} = \pi_1(\tau_1)$, $\mathcal{B} = \pi_2(\tau_2)$ and $\mathcal{C} = \pi_3(\tau_3)$. In addition, we will use the notation $\mathcal{A}_\lambda := \pi_\lambda(\tau_\lambda)$. After a perturbation of \mathcal{K} , we can assume that the projections $\mathcal{A}, \mathcal{B}, \mathcal{C}$ are mutually transverse and self-transverse, with intersections away from the bridge points. In diagrams, our color conventions are that \mathcal{A} consists of red arcs, \mathcal{B} consists of blue arcs, and \mathcal{C} consists of green arcs. A torus diagram for the cubic curve in \mathbb{CP}^2 is given in Figure 2.

The orientation on the tangles induces orientations on the projections. We can therefore interpret $\mathcal{A}, \mathcal{B}, \mathcal{C}$ as oriented 1-chains on T^2 satisfying

$$\partial \mathcal{A} = \partial \mathcal{B} = \partial \mathcal{C}$$

The closed 1-chains

$$\mathcal{S}(K_1) := \mathcal{A} - \mathcal{B} \quad \mathcal{S}(K_2) := \mathcal{B} - \mathcal{C} \quad \mathcal{S}(K_3) := \mathcal{C} - \mathcal{A}$$

are the projections of the oriented links K_1, K_2, K_3 onto the central surface. These projections may be homologically essential in Σ , living in the classes

$$\begin{aligned} [\mathcal{S}(K_1)] &= p_1[\alpha] + q_1[\beta] \\ [\mathcal{S}(K_2)] &= p_2[\beta] + q_2[\gamma] \\ [\mathcal{S}(K_3)] &= p_3[\gamma] + q_3[\alpha] \end{aligned}$$

for some integers $\{p_\lambda, q_\lambda\}$.

We define a secondary sign $\epsilon(v)$ for each bridge point v , according to the cyclic ordering of the incoming shadows. If the three incoming arcs of $\mathcal{A}, \mathcal{B}, \mathcal{C}$ at v are positively cyclically ordered with respect to the orientation on Σ , we set $\epsilon(v) = 1$; otherwise we set $\epsilon(v) = -1$. See Figure 4.

Finally, we will use the following convention to determine over-/undercrossings. Recall we have a Heegaard decomposition $Y_\lambda = H_\lambda \cup -H_{\lambda+1}$. We view Σ from the perspective of the core of $-H_{\lambda+1}$, so that the tangle $\tau_{\lambda+1}$ is in the foreground and τ_λ is in the background.

Thus, the arcs of $\pi_{\lambda+1}(\tau_{\lambda+1})$ always pass over the arcs of $\pi_\lambda(\tau_\lambda)$. In absolute terms, the arcs of \mathcal{B} always pass over the arcs of \mathcal{A} , the arcs of \mathcal{C} always pass over the arcs of \mathcal{B} , and the arcs of \mathcal{A} always pass over the arcs of \mathcal{C} . Using the color conventions of red, blue, and green for $\mathcal{A}, \mathcal{B}, \mathcal{C}$, respectively, we have the convention: *blue over red, green over blue, red over green*.

For self-intersections of $\pi_\lambda(\tau_\lambda)$, the strand further from Σ passes under the strand closer to Σ . The opposite occurs for self-intersections of $\pi_{\lambda+1}(\tau_{\lambda+1})$. Thus, the crossing information for $\pi_\lambda(\tau_\lambda)$ depends on whether the ambient manifold is Y_λ or $Y_{\lambda-1}$. When drawing diagrams, as in Figure 3, we always assume that ambient manifold is Y_λ .

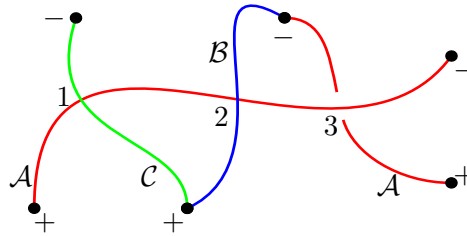


FIGURE 3. An example piece torus diagram. Crossing 1 contributes -1 to the writhe $w(S_3)$. Crossing 2 contributes $+1$ to the writhe $w(S_1)$. Crossing 3 contributes $+1$ to $w(S_1)$ and -1 to $w(S_3)$.

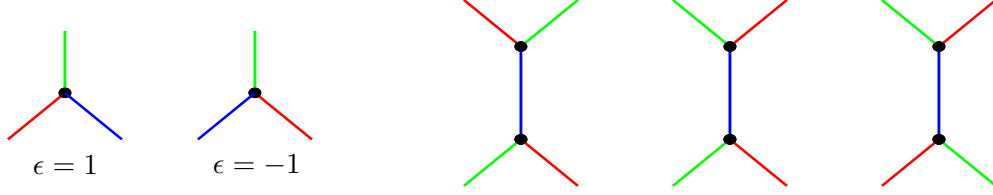


FIGURE 4. (Left) A positive and negative bridge point in the shadow diagram. (Right) A positively twisted, untwisted, and negatively twisted band in the shadow diagram.

2.6. Degree formulas. Let L_λ denote the complex line $\{z_\lambda = 0\}$ in \mathbb{CP}^2 . This complex line intersects the handlebody H_λ along a core B_λ of the solid torus, geometrically dual to the compressing disk bounded by α_λ . We view B_λ as an oriented knot in $H_\lambda \subset Y_\lambda = \partial X_\lambda$, oriented as the boundary of the disk $\mathcal{L}_{\lambda,N} := L_\lambda \cap X_\lambda$. The mirror image with the reverse orientation $-B_\lambda^r$, which is an oriented knot in $-H_\lambda \subset Y_{\lambda-1} = \partial X_{\lambda-1}$, is also the oriented boundary of the disk $\mathcal{L}_{\lambda,S} := L_\lambda \cap X_{\lambda-1}$.

Proposition 2.1. *Let $(\mathbb{CP}^2, \mathcal{K})$ be an immersed, oriented surface in general position with respect to the standard trisection. The degree of \mathcal{K} is given by the following formulas.*

- (1) *Let L_λ be the complex line $\{z_\lambda = 0\}$. Then*

$$d = [L_\lambda] \cdot [\mathcal{K}]$$

where \cdot denotes the intersection pairing on $H_2(\mathbb{CP}^2; \mathbb{Z})$.

- (2) *Let $B_\lambda \subset H_\lambda$ denote the intersection of L_λ with H_λ . Then*

$$d = lk_{Y_\lambda}(K_\lambda, B_\lambda) + lk_{Y_{\lambda-1}}(K_{\lambda-1}, -B_\lambda^r)$$

- (3) *Let $[\alpha_{\lambda-1}], [\alpha_{\lambda+1}]$ denote classes in $H_1(T^2; \mathbb{Z})$. Then*

$$d = \langle \mathcal{S}(K_\lambda), [\alpha_{\lambda+1}] \rangle + \langle [\alpha_{\lambda-1}], \mathcal{S}(K_{\lambda-1}) \rangle$$

where $\langle \cdot, \cdot \rangle$ denotes the intersection pairing on $H_1(T^2; \mathbb{Z})$.

Proof. In \mathbb{CP}^2 , the degree of \mathcal{K} is given by the algebraic intersection number of Σ with any surface of degree 1. We can choose this surface to be L_λ .

The complex line L_λ decomposes as the union $\mathcal{L}_{\lambda,N} \cup \mathcal{L}_{\lambda,S}$. It follows immediately that

$$d = \sum_{x \in L_\lambda \cap \mathcal{K}} \sigma(x) = \sum_{y \in \mathcal{L}_{\lambda,N} \cap \mathcal{D}_\lambda} \sigma(y) + \sum_{y \in \mathcal{L}_{\lambda,S} \cap \mathcal{D}_{\lambda-1}} \sigma(y)$$

where σ denotes the sign of the intersection. The surfaces $(\mathcal{D}_\lambda, K_\lambda)$ and $(\mathcal{L}_{\lambda,N}, B_\lambda)$ are properly embedded in (X_λ, Y_λ) and the surfaces $(\mathcal{D}_{\lambda-1}, K_{\lambda-1})$ and $(\mathcal{L}_{\lambda,S}, -B_\lambda^r)$ are properly embedded in $(X_{\lambda-1}, Y_{\lambda-1})$. Consequently,

$$\sum_{y \in \mathcal{L}_{\lambda,N} \cap \mathcal{D}_\lambda} \sigma(y) = lk_{Y_\lambda}(K_\lambda, B_\lambda) \quad \sum_{y \in \mathcal{L}_{\lambda,S} \cap \mathcal{D}_{\lambda-1}} \sigma(y) = lk_{Y_{\lambda-1}}(K_{\lambda-1}, -B_\lambda^r)$$

and the second formula follows.

Finally, we can compute linking numbers via the intersection pairing on $H_1(\Sigma; \mathbb{Z})$. Let F be a compressing disk bounded by $\alpha_{\lambda+1}$ in $-H_{\lambda+1}$ and extend it into H_λ to obtain a Seifert surface \widehat{F} for

B_λ in Y_λ . By an isotopy, we can assume that there is a one-to-one correspondence between points of $K_\lambda \cap \widehat{F}$ in Y_λ and points of $\alpha_{\lambda+1} \cap \mathcal{S}(K_\lambda)$ in T^2 . Counting with signs shows that

$$lk_{Y_\lambda}(K_\lambda, B_\lambda) = \langle \mathcal{S}(K_\lambda), [\alpha_{\lambda+1}] \rangle.$$

A similar argument shows that

$$lk_{Y_{\lambda-1}}(K_{\lambda-1}, -B'_\lambda) = \langle [\alpha_{\lambda-1}], \mathcal{S}(K_{\lambda-1}) \rangle$$

and the third formula follows from the second. \square

Corollary 2.2. *Let $(\mathbb{CP}^2, \mathcal{K})$ be knotted surface of degree d in bridge position with shadow diagram \mathcal{S} . Then there exist integers p, q, r such that, in $H_1(T^2; \mathbb{Z})$, the links represent the homology classes:*

$$\begin{aligned} [\mathcal{S}(K_1)] &= p \cdot [\alpha] + (d - q) \cdot [\beta] \\ [\mathcal{S}(K_2)] &= q \cdot [\beta] + (d - r) \cdot [\gamma] \\ [\mathcal{S}(K_3)] &= r \cdot [\gamma] + (d - p) \cdot [\alpha] \end{aligned}$$

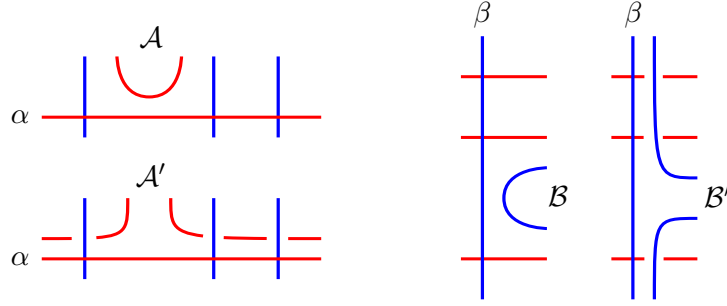
Proof. This follows immediately from Proposition 2.1 since the intersection pairing on $H_1(T^2)$ is non-degenerate. \square

2.7. Bridge stabilization. There is a natural notion of stabilization for surfaces in bridge position that increases the bridge index by 1 [MZ17a]. The only type of stabilization we will need in this paper is what we will call a *mini stabilization*. In dimension 4, a mini-stabilization corresponds to an isotopy given by a finger move of the surface \mathcal{K} through the central surface Σ of the trisection. Specifically, take a neighborhood in \mathcal{K} of an arc of τ_λ and push it towards the central surface. After pushing through Σ , the isotoped surface \mathcal{K} now intersects $X_{\lambda+1}$ in an extra trivial disk. Diagrammatically, this can be seen as creating two bridge points along some arc of the shadow \mathcal{A}_λ and adding a new arc to both $\mathcal{A}_{\lambda+1}$ and $\mathcal{A}_{\lambda-1}$. See Figure 5. It is clear that this corresponds to a bridge stabilization of the links $K_{\lambda-1}$ and K_λ , while introduces an extra unlinked, unknotted component to $K_{\lambda+1}$. Thus, we still have a bridge trisection of \mathcal{K} .



FIGURE 5. A torus diagram depiction of a mini bridge stabilization.

2.8. Braid stabilization. An isotopy of τ_λ that passes through B_λ changes the homology classes represented by $\mathcal{S}(K_{\lambda-1})$ and $\mathcal{S}(K_\lambda)$. In particular, after the isotopy we obtain a new projection \mathcal{A}'_λ such that $[\mathcal{A}_\lambda - \mathcal{A}'_\lambda] = j[\alpha_\lambda]$ in $H_1(T^2)$ for some integer j . We refer to this as a *braid stabilization*. See Figure 6.

FIGURE 6. (Left:) α -stabilization. (Right:) β -stabilization.

Proposition 2.3. *Let $(\mathbb{CP}^2, \mathcal{K})$ be an immersed surface of degree d in general position with torus diagram \mathcal{S} . Then for any integers p, q, r there exists a sequence of braid stabilizations such that the links represent the following homology classes in $H_1(T^2; \mathbb{Z})$:*

$$\mathcal{S}(K_1) = p \cdot [\alpha] + (d - q) \cdot [\beta]$$

$$\mathcal{S}(K_2) = q \cdot [\beta] + (d - r) \cdot [\gamma]$$

$$\mathcal{S}(K_3) = r \cdot [\gamma] + (d - p) \cdot [\alpha]$$

Proof. By Corollary 2.2, we can find some choice of integers p', q', r' . Now perform $p - p'$ α -stabilizations, $q - q'$ β -stabilizations, and $r - r'$ γ stabilizations. \square

2.9. Surface framings. In a torus diagram, we assign a formal writhe to each link projection $\mathcal{S}(K_\lambda)$ as follows. Each $\mathcal{S}(K_\lambda) = \mathcal{A}_\lambda - \mathcal{A}_{\lambda+1}$ is a collection of oriented, self-transverse curves. In addition, at each point self-intersection point we have crossing information and can therefore assign a sign in the standard way. Define the *writhe* $w_\lambda(\mathcal{S})$ as the signed count of crossings of by $\mathcal{S}(K_\lambda)$. The writhe $w_\lambda(\mathcal{S})$ describes the surface framing of K_λ determined by Σ , up to a correction term determined by the homology class of $\mathcal{S}(K_\lambda)$.

Lemma 2.4. *Suppose that $[\mathcal{S}(K_\lambda)] = p \cdot [\alpha_\lambda] + q \cdot [\alpha_{\lambda+1}]$. Then the surface framing on K_λ induced by $\mathcal{S}(K_\lambda)$ is $w_\lambda(\mathcal{S}) + pq$.*

Proof. If $\mathcal{S}(K_\lambda)$ lies in a disk on Σ , then $p = q = 0$ and the surface framing is exactly given by the writhe $w_\lambda(\mathcal{S})$. Furthermore, any isotopy of K_λ that induces a regular homotopy of $\mathcal{S}(K_\lambda)$ preserves the surface framing as well as $w_\lambda(\mathcal{S})$. To obtain the formula, we just need to check that it does not change under braid stabilization.

Isotope K_λ by a single braid stabilization through B_λ and let $\mathcal{S}'(K_\lambda)$ denote the resulting projection. Thus $[\mathcal{S}'(K_\lambda)] - [\mathcal{S}(K_\lambda)] = [\alpha_\lambda]$. This does not change the surface framing but does change the signed count of crossings, as is evident in Figure 6, by

$$w_1(\mathcal{S}') = w_1(\mathcal{S}) - q.$$

Consequently

$$w_1(\mathcal{S}') + (p + 1)q = w_1(\mathcal{S}) - q + pq + q = w_1(\mathcal{S}) + pq.$$

An identical argument shows that the sum $w_1(\mathcal{S}) + pq$ is invariant under braid stabilization passing through $-B_{\lambda+1}^r$ as well. \square

Proposition 2.5. *Let $(\mathbb{CP}^2, \mathcal{K})$ be an immersed surface of degree- d surface in general position with respect to the trisection and with torus diagram \mathcal{S} . Suppose that the projections of the three links of the bridge trisection represent the classes*

$$\begin{aligned} [\mathcal{S}(K_1)] &= p \cdot [\alpha] + (d - q) \cdot [\beta] \\ [\mathcal{S}(K_2)] &= q \cdot [\beta] + (d - r) \cdot [\gamma] \\ [\mathcal{S}(K_3)] &= r \cdot [\gamma] + (d - p) \cdot [\alpha] \end{aligned}$$

in $H_1(\Sigma)$. Then

$$\begin{aligned} \langle \mathcal{S}(K_\lambda), \mathcal{S}(K_{\lambda+1}) \rangle &= d^2 - d(p + q + r) + pq + qr + rp \\ &= w_1(\mathcal{S}) + w_2(\mathcal{S}) + w_3(\mathcal{S}) + \frac{1}{2} \sum_v \epsilon_{\mathcal{S}}(v). \end{aligned}$$

Proof. The computation of the algebraic intersection number $\langle \mathcal{S}(K_\lambda), \mathcal{S}(K_{\lambda+1}) \rangle$ follows immediately since

$$\langle [\alpha], [\beta] \rangle = 1 \quad \text{and} \quad [\gamma] = -[\alpha] - [\beta].$$

In addition, we can also compute the algebraic intersection number $\langle \mathcal{S}(K_\lambda), \mathcal{S}(K_{\lambda+1}) \rangle$ from the torus diagram \mathcal{S} . There are five types of potential contributions: (1) $\mathcal{A} - \mathcal{B}$ crossings, (2) $\mathcal{B} - \mathcal{C}$ crossings, (3) $\mathcal{C} - \mathcal{A}$ crossings, (4) self-intersections of $\mathcal{A}, \mathcal{B}, \mathcal{C}$, and (5) $\mathcal{A}_{\lambda+1}$ -arcs. Contributions may arise from $\mathcal{A}_{\lambda+1}$ arcs because the projections $\mathcal{S}(K_\lambda)$ and $\mathcal{S}(K_{\lambda+1})$ are tangent along these arcs.

The first three contribute to $w_1(\mathcal{S}), w_2(\mathcal{S}), w_3(\mathcal{S})$, respectively, and with our orientation and crossing conventions, the signs agree. The fourth contribute 0 on net. Each self-intersection point of some \mathcal{A}_μ contributes opposite signs to $w_\mu(\mathcal{S})$ and $w_{\mu-1}(\mathcal{S})$ because the crossing data changes.

Finally, the remaining contributions to the algebraic intersection number come from the $\mathcal{A}_{\lambda+1}$ arcs. Let v_1, v_2 be the endpoint of some arc $\mathcal{A}_{\lambda,i}$. If $\epsilon(v_1) = \epsilon(v_2) = 1$, then we can perturb $\mathcal{S}(K_{\lambda+1})$ to add a single positive intersection point. Similarly, if $\epsilon(v_1) = \epsilon(v_2) = -1$, a perturbation yields a negative intersection point. Finally, if $\epsilon(v_1) = -\epsilon(v_2)$, we can perturb $\mathcal{S}(K_{\lambda+1})$ and locally remove any intersection point along the arc. The total contribution over all $\mathcal{A}_{\lambda+1}$ arcs is exactly half the ϵ -count of bridge points. See Figure 4. \square

When the homological data is triple symmetric and the bridge points are positively cyclically oriented, we get the following corollary, which relates the homological self-intersection number of \mathcal{K} , the intersection pairing applied to the shadow \mathcal{S} , the writhe of the shadow \mathcal{S} , and the bridge index.

Corollary 2.6. *Let $(\mathbb{CP}^2, \mathcal{K})$ be a knotted surface of degree- d surface in bridge position with shadow diagram \mathcal{S} . Suppose that the shadows of the three links of the bridge trisection represent the classes*

$$\begin{aligned} [\mathcal{S}(K_1)] &= d \cdot [\alpha] + 0 \cdot [\beta] \\ [\mathcal{S}(K_2)] &= d \cdot [\beta] + 0 \cdot [\gamma] \\ [\mathcal{S}(K_3)] &= d \cdot [\gamma] + 0 \cdot [\alpha] \end{aligned}$$

in $H_1(\Sigma)$ and $\epsilon_{\mathcal{S}}(v) = 1$ for all bridge points. Then

$$d^2 = \langle \mathcal{S}(K_\lambda), \mathcal{S}(K_{\lambda+1}) \rangle = w_1(\mathcal{S}) + w_2(\mathcal{S}) + w_3(\mathcal{S}) - b.$$

Remark 2.7. Lemma 2.4 quantifies the difference between the surface framing of $\mathcal{S}(L_1)$ and the nullhomologous framing in terms of the writhe. Thus, Proposition 2.5 can also be interpreted as a linear constraint on the surface framings of the three links comprising the spine of the surface.

3. TRANSVERSE BRIDGE POSITION

The complex geometry of \mathbb{CP}^2 naturally induces contact structures on each 3-manifold Y_λ of the trisection decomposition.

3.1. The contact structure (S^3, ξ_{join}) . We may view S^3 as the join $S^1 * S^1$ and from this perspective construct the standard tight contact structure on S^3 .

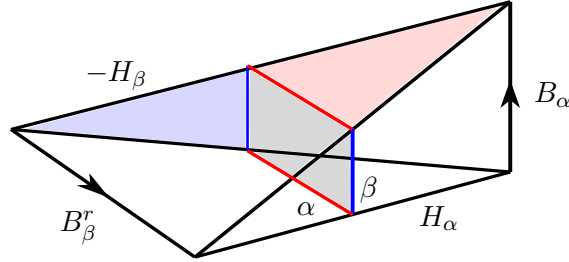


FIGURE 7. S^3 viewed as the join $S^1 * S^1$, obtained by identifying the top and bottom faces and identifying the front and back faces. The Heegaard surface T^2 is shaded in gray. The β curve bounds a blue compressing disk; the α curve bounds a red compressing disk. The oriented edges become the positive Hopf link in S^3 .

Consider $M = [0, 1] \times S^1 \times S^1$ with coordinates (t, x, y) . Choose a smooth, increasing function $h(t) : [0, 1] \rightarrow [0, 1]$ with $h(0) = 0$ and $h(1) = 1$. Define the contact structure

$$\xi_h = \ker \left(\sin \left(\frac{\pi}{2} h(t) \right) dx + \cos \left(\frac{\pi}{2} h(t) \right) dy \right).$$

At $t = 0$, the contact form is dy and at $t = 1$, the contact form is dx , and for $t \in (0, 1)$, the contact planes turn monotonically counter-clockwise through a total angle of $\frac{\pi}{2}$. Up to isotopy, the contact structure ξ_h is independent of the function h . Collapsing at $t = 0$ and $t = 1$, this contact structure descends to the contact structure ξ_{join} on $S^1 * S^1 = S^3$, which is exactly the standard tight contact structure.

Remark 3.1. The expert reader should beware:

- (1) The contact structure (S^3, ξ_{join}) admits an open book decomposition with the positive Hopf link as its binding. However, the Heegaard decomposition obtained from this open book does not agree with the natural Heegaard decomposition here along $\{\frac{1}{2}\} \times T^2$. In particular, the Heegaard surface here is not the union of two pages of the open book decomposition.
- (2) In the standard convention for front diagrams with the contact form $\alpha = dz - ydx$, the vector ∂_y points into the page. However, we will adopt the convention that the vector ∂_t points out of the page. In particular, at $t = 1$ the contact structure has vertical slope and is cooriented to the right (positive x direction, while at $t = 0$ the contact structure has horizontal slope and is cooriented to the top (positive y direction). Here, x and y are the standard coordinates in the page.

3.2. Projections of transverse links. Given a link $L \subset S^1 * S^1$ disjoint from the Hopf link, we can lift L to a link in $M = T^2 \times [0, 1]$ and consider its projection onto the Heegaard surface $\Sigma = \{\frac{1}{2}\} \times T^2$. By abuse of notation, we also refer to this link as L .

Let L be a nullhomologous transverse link in a contact manifold (Y, ξ) and let F be a connected, oriented Seifert surface for L . The *self-linking number* of L with respect to F is a \mathbb{Z} -valued invariant, well-defined up to isotopy through transverse links. The bundle $\xi|_F$ is trivial and so admits a nonvanishing section s . Along L , the section s determines a framing and a pushoff L' in the direction of this framing. The *self-linking number* is defined to be

$$sl(L, F) := lk(L, L').$$

If the Euler class of the contact structure ξ vanishes, then the self-linking number is independent of the surface F .

Proposition 3.2. *Let L be a transverse link in (S^3, ξ_{join}) disjoint from the positive Hopf link $B_\alpha \cup -B_\beta^r$. Lift L to a link in $M = T^2 \times [0, 1]$ and project onto $\{\frac{1}{2}\} \times T^2$. Let \mathcal{D} be the resulting diagram, let $w(\mathcal{D})$ denote the signed count of positive and negative crossings in \mathcal{D} , and let $p[\alpha] + q[\beta]$ be the homology class of L .*

The self-linking number of L is given by the formula

$$sl(L) = w(\mathcal{D}) + pq - p - q.$$

Proof. Choose a Seifert surface $\Sigma \subset S^3$ for L . After multiplying by a nonnegative function, the vector field ∂_t on M descends to a section of ξ_i that vanishes along the Hopf link $B_\alpha \cup -B_\beta^r$. We can use this vector field to compute the self-linking number, provided we add a correction term corresponding to the intersection points $F \cap B_\alpha \cup -B_\beta^r$ as follows. Let L_t denote the framed pushoff of L determined by ∂_t . Then we have

$$\begin{aligned} sl(L, F) &= lk(L, L_t) - \sum_{x \in F \cap H} \sigma(x) \\ &= lk(L, L_t) - (lk(L, B_\alpha) + lk(L, -B_\beta^r)) \\ &= lk(L, L_t) - p - q. \end{aligned}$$

where $\sigma(x)$ denotes the sign of the intersection.

The formula now follows by applying Lemma 2.4 since ∂_t is transverse to $\frac{1}{2} \times T^2$ and therefore determines the surface framing. \square

Remark 3.3. Similar formulas for the classical invariants of Legendrian and transverse knots were obtained in [Dym04, KP11].

Projections of transverse links to Σ satisfy certain geometric conditions.

Proposition 3.4. *Let L be an (oriented) transverse link in (M, ξ_M) with projection \mathcal{D} onto $\Sigma = T^2 \times \{\frac{1}{2}\}$. Then*

- (1) *at each point of \mathcal{D} , the slope of the tangent vector lies in the interval $(-\frac{\pi}{2}, \pi)$, and*
- (2) *there are no positive crossings as in Figure 8.*

Proof. Since the vector field $\frac{\partial}{\partial t}$ is a section of ξ_M , we can project the contact structure to a family of line fields on T^2 . Let $s_0 = (t_0, x_0, y_0)$ be a point on L . Then an oriented tangent vector to L at s_0 must have slope in the interval $(-\frac{\pi}{2} + t_0 \frac{\pi}{2}, \frac{\pi}{2} + t_0 \frac{\pi}{2})$ in order to positively transverse to ξ_M . Letting t_0 range over the interval $[0, 1]$ shows that the tangent vector at any point lies in the range specified

above. Secondly, let s_1, s_2 be two points on T . If the slope at s_1 lies in the interval $(\frac{\pi}{2}, \pi)$ and the slope at s_2 lies in $(-\frac{\pi}{2}, 0)$, then the t -coordinate at s_2 must be greater than the t -coordinate at s_1 . This excludes the crossing in Figure 8. \square

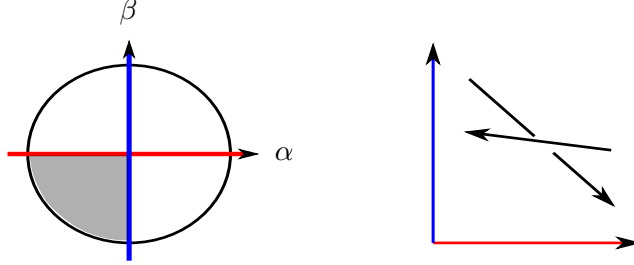


FIGURE 8. (Left:) The excluded slopes, relative to the oriented basis $\{\alpha, \beta\}$ are shaded. (Right:) The excluded positive crossing.

Given the conclusions of Proposition 3.4, we make the following definition.

Definition 3.5. Let $L \subset M_{T^2}$ be a link with a generic projection \mathcal{D} onto the central torus. The diagram \mathcal{D} is *transverse* if it satisfies the conclusions of Proposition 3.4.

Admitting a transverse projection is sufficient to be isotopic to a transverse link with the same projection.

Proposition 3.6. Suppose that L projects to a transverse diagram \mathcal{D} . Then there exists some L' , transverse to ξ and isotopic to L , with the same projection \mathcal{D} .

Proof. Since \mathcal{D} has only allowable slopes, we can build a regular homotopy of L to a transverse link with the same projection simply by increasing or decreasing the t -coordinate of each point on L . Moreover, since \mathcal{D} has no excluded crossings, we can assume this homotopy is in fact an isotopy. \square

3.3. The contact structures $(\hat{Y}_{\lambda,N}, \hat{\xi}_{\lambda,N})$. Recall that in the affine chart obtained by setting $z_{\lambda-1} = 1$, the sector X_λ is exactly the polydisk $\Delta = \{|z_\lambda|, |z_{\lambda+1}| \leq 1\}$. This polydisk can be approximated by a holomorphically convex 4-ball. Specifically, consider the function

$$f_{\lambda,N}(z_\lambda, z_{\lambda+1}) := \frac{1}{N}(|z_\lambda|^2 + |z_{\lambda+1}|^2) + |z_\lambda|^{2N} + |z_{\lambda+1}|^{2N}$$

for some $N \gg 0$.

Lemma 3.7. Let $\hat{X}_{\lambda,N}$ be the compact sublevel set $f_{\lambda,N}^{-1}((-\infty, 1])$ of $f_{\lambda,N}$ for $N \gg 0$.

- (1) For N sufficiently large, the level set $\hat{Y}_{\lambda,N} := \partial \hat{X}_{\lambda,N} = S^3$ is C^0 -close to Y_λ .
- (2) Let U be a fixed open neighborhood of the central surface Σ . For N sufficiently large, the level set $\hat{Y}_{\lambda,N}$ is C^∞ -close to Y_λ outside U .
- (3) $\hat{X}_{\lambda,N}$ is a Stein domain contained in the interior of X_λ .
- (4) The field $\hat{\xi}_{\lambda,N}$ of complex tangencies to $\hat{Y}_{\lambda,N}$ is the standard tight contact structure.

Proof. For large N , the function $(f_{\lambda,N})^{\frac{1}{2N}}$ is a perturbation of the L^{2N} -norm. Thus, the level set $f_{\lambda,N}^{-1}(1)$ is a perturbation of the unit circle in \mathbb{C}^2 with respect to the L^{2N} -norm. These level sets then must converge to Y_λ , which is the unit circle with respect to the L^∞ -norm. This convergence is uniform outside a fixed open neighborhood of Σ . Finally, the function $f_{\lambda,N}$ is strictly plurisubharmonic for all $N > 1$, therefore its sublevel sets are Stein. Therefore the field of complex tangencies along its boundary is a contact structure. The boundary is S^3 and the contact structure must be the unique tight contact structure. \square

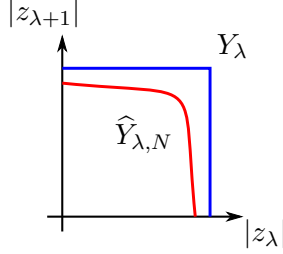


FIGURE 9. As $N \rightarrow \infty$, the level set $\hat{Y}_{\lambda,N}$ approaches Y_λ .

3.4. Transverse bridge position. The 4-dimensional picture above motivates the introduction of transverse bridge position and transverse shadow diagrams in this section. Roughly speaking, a surface $(\mathbb{CP}^2, \mathcal{K})$ is in transverse bridge position if it is in bridge position with respect to the standard genus 1 trisection and it intersects each $(\hat{Y}_i, \hat{\xi}_i)$ in a transverse unlink. Given the above observation about the limiting behavior of $\hat{\xi}_i$, we make the following definition.

A surface $(\mathbb{CP}^2, \mathcal{K})$ has *complex bridge points* if for each point $[x : y : 1] \in \mathcal{K} \cap \Sigma$, the surface \mathcal{K} locally agrees with the projective line $\left\{ \frac{\zeta}{x}z_1 + \frac{\zeta^2}{y}z_2 + z_3 = 0 \right\}$ for some primitive 3rd-root of unity ζ .

Definition 3.8. A knotted surface $(\mathbb{CP}^2, \mathcal{K})$ is *geometrically transverse* if

- (1) \mathcal{K} is in general position with respect to the standard trisection,
- (2) \mathcal{K} has complex bridge points, and
- (3) each tangle $\tau_\lambda = \mathcal{K} \cap H_\lambda$ is positively transverse to the foliation of H_λ by holomorphic disks.

Furthermore, if $(\mathbb{CP}^2, \mathcal{K})$ is geometrically transverse and in bridge position, we say that it is in *transverse bridge position*.

Proposition 3.9. *Let $(\mathbb{CP}^2, \mathcal{K})$ be in general position with respect to the standard trisection*

- (1) *If \mathcal{K} is geometrically transverse, then for N sufficiently large, the intersection $\hat{K}_\lambda := \mathcal{K} \cap \hat{Y}_{\lambda,N}$ is a transverse link.*
- (2) *If \mathcal{K} is in transverse bridge position, then for N sufficiently large, the intersection $\hat{K}_\lambda := \mathcal{K} \cap \hat{Y}_{\lambda,N}$ is a transverse unlink.*

Proof. By assumption, the surface \mathcal{K} has complex bridge points. Thus, we can choose some $\epsilon > 0$ such that within the open set

$$U_\epsilon := \{|1 - |z_1|| < \epsilon, |1 - |z_2|| < \epsilon\}$$

the surface \mathcal{K} agrees with a collection of complex lines. Furthermore, by Lemma 3.7, we can choose N such that outside of U_ϵ the level set $\hat{Y}_{\lambda,N}$ is C^∞ -close to Y_λ .

The surface \mathcal{K} is geometrically transverse, hence it is transverse to the foliation of $Y_\lambda \setminus U_\epsilon$ by holomorphic disks. Since $\hat{Y}_{\lambda,N}$ is C^∞ -close to Y_λ outside U_ϵ , we can assume that \mathcal{K} remains transverse to hypersurface $\hat{Y}_{\lambda,N}$ and positively transverse to its field of complex tangencies on $\hat{Y}_{\lambda,N}$ outside U_ϵ . In other words, outside U_ϵ , the intersection \hat{K}_λ is a 1-manifold that is positively transverse to the contact structure $\hat{\xi}_{\lambda,N}$ — i.e. a tranverse link.

To complete the proof, we need to check that these properties also hold within U_ϵ . In polar coordinates, we can write the function as

$$f_{\lambda,N}(r_1, \theta_1, r_2, \theta_2) = \frac{1}{N}(r_1^2 + r_2^2) + r_1^{2N} + r_2^{2N}$$

Its gradient with respect to the standard metric is therefore

$$\nabla f_{\lambda,N} = \frac{2}{N}(r_1 \partial_{r_1} + r_2 \partial_{r_2}) + 2N(r_1^{2N-1} \partial_{r_1} + r_2^{2N-1} \partial_{r_2})$$

If $w = (r_1 e^{i\theta_1}, r_2 e^{i\theta_2})$ is a point in $\hat{Y}_{\lambda,N}$, then the complex line generated by $\nabla f_{\lambda,N}$ at w has slope

$$\left[\left(\frac{2}{N} r_1 + 2N r_1^{2N-1} \right) e^{i\theta_1} : \left(\frac{2}{N} r_2 + 2N r_2^{2N-1} \right) e^{i\theta_2} \right]$$

and therefore the contact tangency to $\hat{Y}_{\lambda,N}$ at w is the complex line of slope

$$\left[- \left(\frac{2}{N} r_2 - 2N r_2^{2N-1} \right) e^{i\theta_2} : \left(\frac{2}{N} r_1 + 2N r_1^{2N-1} \right) e^{i\theta_1} \right]$$

Now suppose w is a point in $\mathcal{K} \cap \hat{Y}_{\lambda,N} \cap U_\epsilon$. The tangent plane to \mathcal{K} at w is the complex line of slope $[x\zeta : y]$, where x, y have unit norm, ζ is a primitive 3rd-root of unity, and $|x - e^{i\theta_1}| < \epsilon$ and $|y - e^{i\theta_2}| < \epsilon$. We can now see that $\left(\hat{\xi}_{\lambda,N} \right)_w \neq T_w \mathcal{K}$, as they always have different complex slopes. This implies that \mathcal{K} intersects $\hat{Y}_{\lambda,N}$ transversely and since complex lines intersect positively, it also implies that \hat{K}_λ is positively transverse to $\hat{\xi}_{\lambda,N}$.

Part (2) follows immediately from Part (1), since if \mathcal{K} is in bridge position, it intersects each Y_λ , and therefore $\hat{Y}_{\lambda,N}$, along an unlink. \square

3.5. Total self-linking number. When $(\mathbb{CP}^2, \mathcal{K})$ is geometrically transverse, the total self-linking numbers of the three links $\hat{K}_1, \hat{K}_2, \hat{K}_3$ can be computed from a torus diagram and is completely determined by algebraic information of \mathcal{K} .

First, we can identify $\hat{Y}_{\lambda,N}$ with Y_λ via projection. Define a map $\Phi_\lambda : \mathbb{C}^2 \setminus \{0\} \rightarrow Y_\lambda$ by setting

$$\Phi_\lambda : (r_1 e^{i\theta_1}, r_2 e^{i\theta_2}) \mapsto \begin{cases} \left(e^{i\theta_1}, \frac{r_2}{r_1} e^{i\theta_2} \right) & \text{if } r_1 \geq r_2 \\ \left(\frac{r_1}{r_2} e^{i\theta_1}, e^{i\theta_2} \right) & \text{if } r_1 \leq r_2 \end{cases}$$

The restriction of Φ_λ to $\hat{Y}_{\lambda,N}$ is a homeomorphism. For N sufficiently large, let ξ_λ be the contact structure on Y_λ obtained by pushing forward $\hat{\xi}_{\lambda,N}$ via Φ_λ .

Lemma 3.10. *Let $(\mathbb{CP}^2, \mathcal{K})$ be a geometrically transverse surface. The link K_λ is a transverse link in (Y_λ, ξ_λ) and*

$$sl(K_\lambda) = sl(\hat{K}_\lambda).$$

Proof. We can assume the link $\Phi_\lambda(\widehat{K}_\lambda)$ is C^1 -close to K_λ . This implies that K_λ is transverse to ξ_λ and that it is transversely isotopic to $\Phi_\lambda(\widehat{K}_\lambda)$. Thus, the self-linking numbers of \widehat{K}_λ , $\Phi_\lambda(\widehat{K}_\lambda)$ and K_λ agree. \square

Next, we identify (Y_λ, ξ_λ) with (S^3, ξ_{join}) in order to compute self-linking numbers from a torus diagram. There is an obvious identification of Y_λ with $S^1 * S^1$ defined in coordinates by setting

$$x = \theta_\lambda \quad y = \theta_{\lambda+1} \quad t = \begin{cases} \frac{r_\lambda}{2} & \text{if } r_\lambda \leq 1 \\ 1 - \frac{r_\lambda}{2} & \text{if } r_\lambda \geq 1 \end{cases}$$

Consequently, we can identify $\widehat{Y}_{\lambda,N}$ with $S^1 * S^1$ by setting

$$x = \theta_\lambda \quad y = \theta_{\lambda+1} \quad t = \begin{cases} \frac{r_\lambda}{2} & \text{if } r_\lambda \leq 1 \\ 1 - \frac{r_\lambda}{2} & \text{if } r_\lambda \geq 1 \end{cases}$$

We can also write r_2 as a monotonically decreasing function of r_1 and therefore view t as a monotonically increasing function of r_1 as well.

Lemma 3.11. *There are contactomorphisms*

$$(\widehat{Y}_{\lambda,N}, \widehat{\xi}_{\lambda,N}) \cong (Y_\lambda, \xi_\lambda) \cong (S^3, \xi_{join})$$

Proof. In radial coordinates, the standard symplectic form on \mathbb{C}^2 is $\omega_{std} = r_1 dr_1 \wedge d\theta_1 + r_2 dr_2 \wedge d\theta_2$. Therefore, the 1-form

$$\alpha_{\lambda,N} = \iota_{\nabla f_{\lambda,N}} \omega_{std} = \left(\frac{2}{N} r_1^2 + 2N r_1^{2N} \right) d\theta_1 + \left(\frac{2}{N} r_2^2 + 2N r_2^{2N} \right) d\theta_2$$

is a contact form defining $\widehat{\xi}_{\lambda,N}$. We can now define a function $h(t)$ such that

$$h(t(r_1)) = \frac{2}{\pi} \arctan \left(\frac{\frac{2}{N} r_1^2 + 2N r_1^{2N}}{\frac{2}{N} r_2^2 + 2N r_2^{2N}} \right)$$

The function $h(t)$ is monotonically increasing in t , with $h(0) = 0$ and $h(1) = 1$. Thus, pulling back $\alpha_{\lambda,N}$ to $S^1 * S^1$ defines ξ_{join} . \square

Proposition 3.12. *Let $(\mathbb{CP}^2, \mathcal{K})$ be a geometrically transverse, oriented surface of degree $d > 0$ and bridge index b . Let $\widehat{K}_\lambda = \mathcal{K} \cap \widehat{Y}_{\lambda,N}$ for N sufficiently large. Then*

$$sl(\widehat{K}_1) + sl(\widehat{K}_2) + sl(\widehat{K}_3) = d^2 - 3d - b.$$

Proof. By Lemma 3.10, it suffices to compute the total self-linking numbers of K_1, K_2 and K_3 . The identification of Y_λ with $S^1 * S^1$ commutes with the projection maps required to apply the formula of Proposition 3.2.

By Corollary 2.2, the three links have diagrams on the torus representing the classes

$$\begin{aligned} [\mathcal{S}(K_1)] &= p[\alpha] + (d - q)[\beta] \\ [\mathcal{S}(K_2)] &= q[\beta] + (d - r)[\gamma] \\ [\mathcal{S}(K_3)] &= r[\gamma] + (d - p)[\alpha] \end{aligned}$$

for some p, q, r . The self-linking formula (Proposition 3.2) yields

$$\begin{aligned} sl(K_1) &= w_1(\mathcal{S}) + p(d - q) - p - (d - q) \\ sl(K_2) &= w_2(\mathcal{S}) + q(d - r) - q - (d - r) \\ sl(K_3) &= w_3(\mathcal{S}) + r(d - p) - r - (d - p) \end{aligned}$$

Adding all three together, we obtain

$$sl(K_1) + sl(K_2) + sl(K_3) = w_1(\mathcal{S}) + w_2(\mathcal{S}) + w_3(\mathcal{S}) + d(p + q + r) - 3d - (pq + qr + rp).$$

Conversely, from Proposition 2.5 we also know that

$$w_1(\mathcal{S}) + w_2(\mathcal{S}) + w_3(\mathcal{S}) = -d(p + q + r) + (pq + qr + rp) + d^2 - b.$$

Substituting this into the previous equation yields the required equality. \square

An easy corollary is that any surface in transverse bridge position satisfies the adjunction inequality.

Theorem 3.13. *Let $(\mathbb{CP}^2, \mathcal{K})$ be an oriented, connected, smoothly embedded surface of degree $d \geq 0$. Suppose that $(\mathbb{CP}^2, \mathcal{K})$ is in transverse bridge position. Then*

$$\chi(\mathcal{K}) \leq 3d - d^2.$$

Proof. Since \mathcal{K} is in transverse bridge position, each K_λ is the c_λ -component unlink. Thus the Bennequin bound implies that $sl(K_\lambda) \leq -c_\lambda$. Summing over the three components and applying the formula of Proposition 3.12, we obtain the inequality

$$d^2 - 3d - b \leq -c_1 - c_2 - c_3$$

or equivalently

$$3d - d^2 \geq c_1 + c_2 + c_3 - b = \chi(\mathcal{K}).$$

\square

4. ALGEBRAIC TRANSVERSE BRIDGE POSITION

4.1. Algebraic transversality. Let $(\mathbb{CP}^2, \mathcal{K})$ be in general position with respect to the standard trisection. Recall that \mathcal{K} is geometrically transverse if each oriented tangle τ_λ is positively transverse to the foliation of H_λ by holomorphic disks. We have polar coordinates $(r_{\lambda+1}, \theta_\lambda, \theta_{\lambda+1})$ on H_λ . The hyperplane field tangent to the foliation is the kernel of the 1-form $d\theta_{\lambda+1}$. Therefore, the surface is geometrically transverse if and only if for each λ we have that $d\theta_\lambda(\tau'_\lambda)$ is everywhere positive.

Definition 4.1. A surface $(\mathbb{CP}^2, \mathcal{K})$ is *algebraically transverse* if, for each λ and each component $\tau_{\lambda,j}$ of τ_λ , we have that

$$\int_{\tau_{\lambda,j}} d\theta_\lambda > 0.$$

An algebraically transverse surface in bridge position is in *algebraically transverse bridge position*.

Clearly, if $(\mathbb{CP}^2, \mathcal{K})$ is geometrically transverse, it is algebraically transverse. We will also refer to a fixed tangle $(H_\lambda, \tau_\lambda)$ as geometrically or algebraically transverse if it satisfies the criteria.

Lemma 4.2. *Let $(\mathbb{CP}^2, \mathcal{K})$ be in algebraically transverse bridge position. Then \mathcal{K} is regularly homotopic through algebraically transverse surfaces to a geometrically transverse surface.*

Proof. An algebraically transverse tangle is regularly homotopic, through algebraically transverse tangles to a geometrically transverse tangle. Given such a homotopy of some τ_λ , we can extend this to a regular homotopy of the surface \mathcal{K} . \square

Remark 4.3. It is useful to note that homotoping τ_λ through a crossing change corresponds to a finger move of the surface \mathcal{K} .

4.2. Isotopy to algebraic transversality. Every essential, oriented, embedded surface in \mathbb{CP}^2 is isotopic to a surface in algebraically transverse bridge position.

Proposition 4.4. *Let $(\mathbb{CP}^2, \mathcal{K})$ be an embedded, oriented, connected surface of positive degree. Then \mathcal{K} can be isotoped into algebraically transverse bridge position.*

Proof. We will fix absolute coordinates and work in the coordinate chart $z_3 = 1$. Then we have polar coordinates

$$z_1 = r_1 e^{ix} \quad r_2 e^{iy}$$

in this chart that induce coordinates $x, y \in [0, 1]$ on the central surface Σ . We can assume that the intersection of \mathcal{K} with the spine of the trisection lies in this coordinate chart and therefore evaluate algebraic transversality in these coordinates. Recall that the foliation of H_λ by holomorphic disks is determined by a 1-form $d\theta_{\lambda+1}$. In the current coordinates, these 1-forms are

$$d\theta_2 = dy \quad d\theta_3 = -dx \quad d\theta_1 = dx - dy$$

By Theorem 1.8, we can assume \mathcal{K} is in bridge position. Thus, each tangle τ_λ is boundary-parallel and we can assume that each projection $\pi_\lambda(\tau_\lambda)$ is a collection of embedded arcs.

First, we standardize the torus diagram with respect to K_1 . Since K_1 is the unlink with c_1 components, there is a sequence of handle slides and bridge disk slides so that $\mathcal{S}(K_1)$ is embedded and with each component isotopic in T^2 to α and with the same orientation. Handleslide \mathcal{C} over γ to ensure that in homology

$$\begin{aligned} [\mathcal{S}(K_1)] &= c_1[\alpha] + 0[\beta] \\ [\mathcal{S}(K_2)] &= d[\beta] + 0[\gamma] \\ [\mathcal{S}(K_3)] &= d[\gamma] + (d - c_1)[\alpha] \end{aligned}$$

We can assume that for any $\epsilon > 0$, each component of $\mathcal{S}(K_1)$ lies in an open annulus $S^1 \times (y_0, y_0 + \epsilon)$ and that these annuli are pairwise disjoint. Within each annulus, isotope so that each \mathcal{B} -arc has slope -1 . Furthermore, we can assume that, projecting the \mathcal{B} -arcs onto the curve $0 \times S^1$, they are nested: for any pair of arcs $\mathcal{B}_i, \mathcal{B}_j$, either the endpoints of \mathcal{B}_i are contained in the interval between the endpoints of \mathcal{B}_j , or vice versa. Also, by a perturbation, we can assume that each bridge point has a unique x and a unique y coordinate. Since the height of the annulus is ϵ , the length of the β arcs is at most $\sqrt{2}\epsilon$ and their width in the horizontal direction is at most ϵ . Consequently, we must have that

$$c_1 - b\epsilon < \int_{\mathcal{A}} dx < c_1.$$

By construction, we have that

$$\int_{\mathcal{B}} dx \approx \int_{\mathcal{B}} dy \approx 0,$$

so we can therefore conclude that

$$\begin{aligned} \int_{\mathcal{A}} dx &\approx c_1 & \int_{\mathcal{C}} dx &\approx d \\ \int_{\mathcal{A}} dy &\approx 0 & \int_{\mathcal{C}} dy &\approx -d \end{aligned}$$

In particular, we have that $\Gamma := \int_{\mathcal{C}} (dx - dy) \approx 2d \gg 0$. The multiarc \mathcal{C} determines a vector $\bar{\mathcal{C}} \in \mathbb{R}^b$, whose i^{th} coordinate is $\int_{\mathcal{C}_i} (dx - dy)$. This vector lies in the hyperplane $P_{\Gamma} := \{x_1 + \cdots + x_b = \Gamma\}$.

Let \mathcal{A}_i be some arc of \mathcal{A} and let $\mathcal{C}_{i_1}, \mathcal{C}_{i_2}$ be the incident arcs at the endpoints. Translation in the y -direction of the entire arc \mathcal{A}_i by M preserves the fact that \mathcal{A}_i is algebraically transverse, while increasing $\int_{\mathcal{C}_{i_1}} (dx - dy)$ by M and decreasing $\int_{\mathcal{C}_{i_2}} (dx - dy)$ by M . We thus translate the vector $\bar{\mathcal{C}}$ in P_{Γ} by $M(e_{i_1} - e_{i_2})$. Similarly, let \mathcal{B}_j be some arc of \mathcal{B} and $\mathcal{C}_{j_1}, \mathcal{C}_{j_2}$ the incident arcs. Each horizontal translation of \mathcal{B}_j by M also translates $\bar{\mathcal{C}}$ by $M(e_{j_1} - e_{j_2})$.

The spine of Σ is connected, since Σ is connected, so the collection of vectors $\{e_{i_1} - e_{i_2}, e_{j_1} - e_{j_2}\}$ span the subspace $\{x_1 + \cdots + x_n = 0\}$. We can therefore translate $\bar{\mathcal{C}}$ to any point in P_{Γ} by vertical translation of \mathcal{A} -arcs and horizontal translation of \mathcal{B} -arcs. In particular, since $\Gamma > 0$, we can assume that $\bar{\mathcal{C}}$ lies in the positive orthant — i.e. that \mathcal{C} is algebraically transverse. \square

4.3. Braiding tangles in H_{λ} . Let M be an oriented 3-manifold with $\partial M = T^2$. A *relative open book decomposition* on M is a pair (B, ρ) satisfying:

- (1) the *binding* B is an oriented link,
- (2) $\rho : M \setminus B \rightarrow S^1$ is a fibration,
- (3) the restriction $\rho|_{\partial M} : \partial M \rightarrow S^1$ is a fibration,
- (4) the closure of each fiber $\rho^{-1}(\theta)$ is a compact, oriented surface F_{θ} , whose boundary is the union of B with a simple closed curve in ∂M .

The surface $\{F_{\theta}\}$ are the *pages* of the open book decomposition. An oriented tangle (M, τ) is *braided* with respect to a relative open book (B, π) if the tangle is everywhere positively transverse to the pages. In particular, the tangle is disjoint from the binding B .

On each solid torus H_{λ} of the trisection of \mathbb{CP}^2 , we construct a specific relative open book decomposition as follows. Recall that we have polar coordinates $(r_{\lambda+1}, \theta_{\lambda}, \theta_{\lambda+1})$. The binding is the core circle $B_{\lambda} := \{r_{\lambda+1} = 0\}$. On the complement of B_{λ} , we have a fibration

$$\rho_{\lambda} : (r_{\lambda+1}, \theta_{\lambda}, \theta_{\lambda+1}) \mapsto \theta_{\lambda}.$$

The pair $(B_{\lambda}, \rho_{\lambda})$ is then a relative open book decomposition of H_{λ} .

Adapting the proof of Alexander's Theorem, we can braid any tangle with respect to this open book decomposition.

Proposition 4.5. *Let $(H_{\lambda}, \tau_{\lambda})$ be a tangle. There is an isotopy of τ_{λ} such that it is braided with respect to the relative open book decomposition $(B_{\lambda}, \rho_{\lambda})$.*

Thus, we now have two notions of positivity for tangles in H_{λ} : geometric transversality and braiding. These correspond to two distinct ways of foliating H_{λ} and $H_{\lambda} \setminus B_{\lambda}$. See Figure 10.

The following lemma will be useful in the sequel.

Lemma 4.6. *Mini bridge stabilization along a geometric transverse, braided arc preserves geometric transversality of all three tangles τ_1, τ_2, τ_3 .*

Proof. The proof is Figure 5. \square

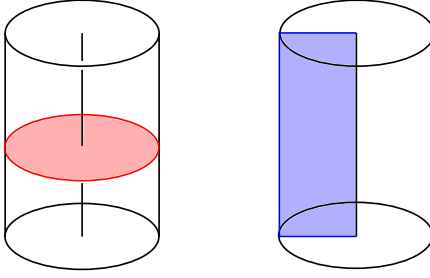


FIGURE 10. (Left) Foliation of H_λ by holomorphic disks. (Right) A relative open book decomposition of H_λ .

4.4. Simple clasps. The prototypical example of a tangle in H_λ that is algebraically transverse and braided, but not geometrically transverse, is the simple clasp in Figure 11. Each of the two strands τ_1, τ_2 can individually be isotoped to be geometrically transverse, but not both simultaneously.

In fact, these clasps are the entire obstruction to isotoping a braided, algebraically transverse tangle τ_λ into a geometrically transverse tangle. In the former, each arc τ_i is isotopic to an arc v_i that projects to a straight line of positive slope on T^2 . By ‘pulling tight’, we can attempt to make τ geometrically transverse by moving each τ_i towards v_i . The obstruction is clearly a collection of clasps. We can then apply mini bridge stabilizations to separate the clasps from one another.

Definition 4.7. A *simple clasp* is a tangle τ in H_λ consisting of two arcs τ_1, τ_2 in τ and a Whitney disk W satisfying

- (1) τ is algebraically transverse and braided, with τ_1 geometrically transverse;
- (2) the Whitney disk W intersects τ_1 transversely in a single point;
- (3) the boundary of W is the union of two arcs $\hat{\tau}_2$ and \hat{v}_2 , where $\hat{\tau}_2$ is a connected subarc of τ_2 and \hat{v}_2 is a geometrically transverse arc.

In addition, we define the *degree* of a simple clasp to be the maximum cardinality of $\pi^{-1} \circ \pi(x)$ for any $x \in W$. An example of a simple clasp of degree 3 is given in Figure 12.

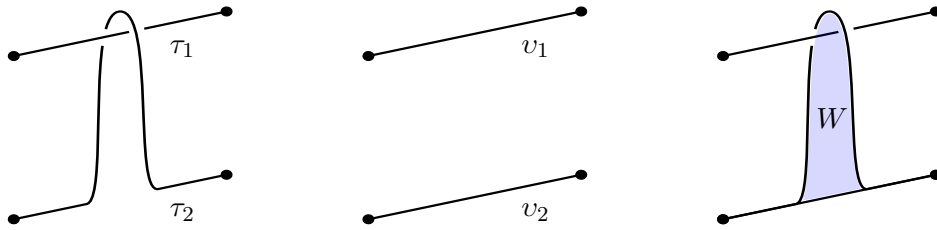


FIGURE 11. (Left) A simple clasp $\tau = \tau_1 \cup \tau_2$. (Middle) A simple clasp τ is homotopic to geometrically transverse tangle $v = v_1 \cup v_2$. (Right) The Whitney disk W directs the homotopy from τ to v .

Proposition 4.8. *Let τ be a tangle in H_λ that is algebraically transverse and braided. Then by a sequence of isotopies and mini bridge stabilizations, we can assume that each arc of τ is either*

- (1) *geometrically transverse and braided, or*
- (2) *one of two arcs in a simple clasp.*

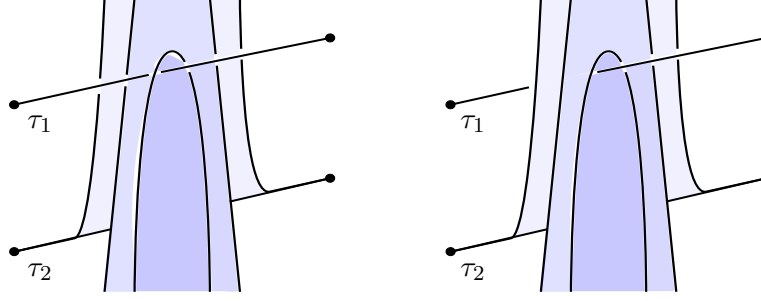


FIGURE 12. (Left) A simple clasp of degree 3. (Right) This clasp is not simple, as the Whitney disk intersects τ_1 in three points.

Proof of Proposition 4.8. As described above, we can achieve the proposition by ‘pulling tight’ and then stabilizing. However, we should think of the tangle as living in $T^2 \times I = H_\lambda \setminus \nu(B_\lambda)$, which is not simply-connected. Therefore, there is some subtlety in the fact that arcs may wind around the torus before clasping. We therefore give a careful exposition of this procedure.

Let τ_i be an arc of τ and choose a lift $\hat{\tau}_i$ to $\mathbb{R}^2 \times I$. Let \hat{v}_i be the arc obtained by isotoping $\hat{\tau}_i$ in the vertical direction until its projection to \mathbb{R}^2 is a straight line and let v_i be the image of \hat{v}_i in $T^2 \times I$. By a C^0 perturbation at the bridge points, we can assume the union $v = \cup\{v_i\}$ is embedded in $T^2 \times I$. By a vertical isotopy of τ in $T^2 \times I$, we can assume that each point of each arc $\hat{\tau}_i$ has greater y -coordinate

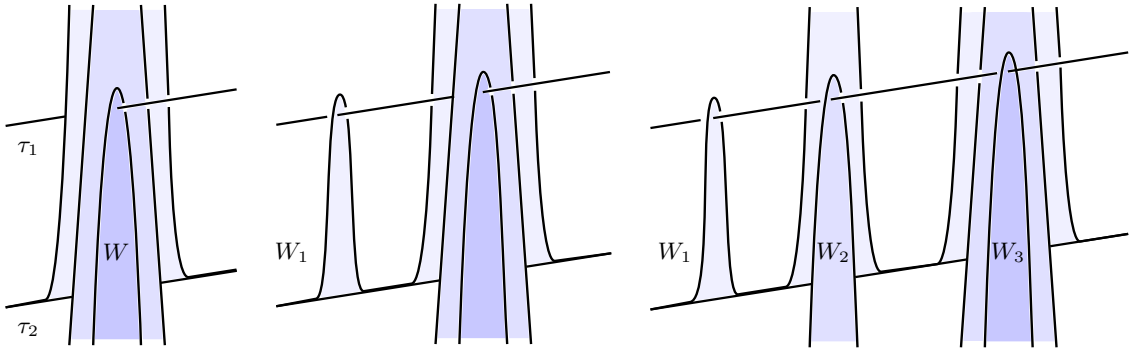


FIGURE 13. (Left) Initially, W is a Whitney disk that intersects τ_1 in three points. (Middle) By an isotopy that projects to a Reidemeister II move, we can split off a Whitney disk W_1 that intersects τ_1 once. (Right) Repeating, we can split W into three Whitney disks, leaving three simple clasps.

in $\mathbb{R}^2 \times I$ that its corresponding point in \widehat{v}_i . Finally, we can assume that the projection of τ to the annulus $S^1 \times I$, obtained by forgetting the y -coordinate, is generic with a finite number of transverse double points.

Now, by a vertical isotopy we can pull the tangle tight by isotoping τ_i in the negative y -direction until it agrees with v_i . Clearly, the only potential obstructions lie above the crossings in the projection to $S^1 \times I$. We can now assume that τ and v agree outside an arbitrarily small neighborhood of these potential obstructions. Let τ_i, τ_j be two arcs that project to a crossing. Let p_i, q_j denote the preimages of the crossing in τ_i and τ_j , respectively. (Note that we may have $i = j$, provided that the points p_i, q_j are distinct). Choose lifts $\widehat{\tau}_i, \widehat{\tau}_j$ such that the difference between the y -coordinate of $\widehat{\tau}_i$ at p_i and the y -coordinate of $\widehat{\tau}_j$ at q_j is some positive Δ between 0 and 2π . Finally, set R_i to be the difference between the y -coordinates of $\widehat{\tau}_i$ and \widehat{v}_i at p_i and similarly set S_i to be the difference between the y -coordinates of $\widehat{\tau}_j$ and \widehat{v}_j at q_j .

We now have three cases:

- (1) if $R_i - \Delta < S_j < R_i + 2\pi - \Delta$, then we can simultaneously isotope τ_i to agree with v_i and τ_j to agree with v_j .
- (2) if $S_j < R_i - \Delta$, then to isotope τ_i to v_i we must homotope it through τ_j at least once. In fact, the number of times we must pass τ_i through τ_j is exactly

$$k := \lceil R_i - \Delta - S_j \rceil.$$

- (3) if $S_j > R_i + 2\pi - \Delta$, then to isotope τ_j to v_j we must homotope it through τ_i at least once. Again, the number of times we must pass τ_j through τ_i is exactly

$$k := \lceil S_j - R_i - 2\pi + \Delta \rceil.$$

Without loss of generality, by reordering the arcs τ_i, τ_j we can assume we are in case (2). We isotope τ_j to agree with v_j and isotope τ_i as far as possible until it locally forms a clasp with τ_j as in Figure 11. The vertical lines between corresponding points in τ_i and v_i comprise a Whitney disk W , which we can perturb to be embedded. An example with $k = 3$ is given on the right of Figure 12.

Note that W intersects τ_j exactly k times, once for each crossing change necessary to isotope τ_i to v_i . Thus we do not yet have simple clasps. However, by an isotopy and mini stabilizations, we can replace this tangle with k simple clasps, one of each degree from 1 to k . Choose $k - 1$ properly embedded arcs that cut W into k disks, each containing one intersection point with τ_j . Isotope τ_i along these arcs to agree with v_i . This splits W into k disks, each corresponding to a single simple clasp. See Figure 13. \square

5. RIBBON-BENNEQUIN INEQUALITY

To prove the adjunction inequality, we need to extend the ribbon-Bennequin inequality to transverse links in $\#_k(S^1 \times S^2, \xi_{std})$.

Let K be a Legendrian knot in (M, ξ) . In any neighborhood of K , we can find a tubular neighborhood $\nu(K)$ and a contactomorphism that identifies $\nu(K)$ with a neighborhood of the 0-section in $J^1(S^1)$. This identification determines a framing of K , called the *contact framing*. Now perform Dehn surgery on M by removing $\nu(K)$ and regluing it along some new slope. If the surgery slope is ± 1 relative to the contact framing, there is a tight contact structure on $S^1 \times D^2$, unique up to isotopy, so that the contact structure ξ , restricted to $M \setminus \nu(K)$, extends across the solid torus. Let $(M_{\pm}(K), \xi_{\pm}(K))$ denote the resulting contact manifolds. We refer to $(M_{-}(K), \xi_{-}(K))$ as *Legendrian surgery* along K .

The following is well-known and can be proven using convex surface theory.

Proposition 5.1. *Let U be a k -component Legendrian link in $\#_k S^1 \times S^2$ whose i^{th} -component is smoothly isotopic to $S^1 \times \{pt\}$ in the i^{th} -factor. The result of Legendrian surgery on U is (S^3, ξ_{std}) .*

Lemma 5.2. *Let L be a transverse link in $\#_k(S^1 \times S^2, \xi_{std})$ that bounds a ribbon surface F . There exists a transverse link L' in (S^3, ξ_{std}) that bounds a ribbon surface F' such that $sl(L) = sl(L')$ and $\chi(F) = \chi(F')$.*

Proof. Let U be the k -component link in $\#_k S^1 \times S^2$ whose i^{th} -component represents $S^1 \times \{pt\}$ in the i^{th} -factor. By an isotopy, we can assume that U is disjoint from the ribbon surface F and then Legendrian realize it by a C^0 -small perturbation. By Proposition 5.1, the result of Legendrian surgery along U is (S^3, ξ_{std}) . We can perform Legendrian surgery in an arbitrary neighborhood of U . In particular, the neighborhood can be assumed disjoint from L and F . Let L', F' be the images of L, F after Legendrian surgery. Note that we can resolve the self-intersections of F to obtain a Seifert surface of L in an arbitrary neighborhood of F . Using this Seifert surface to compute the self-linking number before and after surgery, we see that $sl(L) = sl(L')$. \square

Theorem 5.3. *Let L be a transverse link in $\#_k(S^1 \times S^2, \xi_{std})$ and let F be a ribbon surface bounded by L . Then*

$$sl(L) \leq -\chi(F).$$

Proof. If the pair L, F violates the ribbon-Bennequin inequality in $\#_k(S^1 \times S^2, \xi_{std})$, then by Lemma 5.2, we can find a pair L', F' in (S^3, ξ_{std}) that violates Theorem 1.2. \square

6. ADJUNCTION INEQUALITY

Let $(\mathbb{CP}^2, \mathcal{K})$ be a surface satisfying the conclusions of Proposition 4.8. Specifically, \mathcal{K} is in algebraically transverse bridge position and each arc of each oriented tangle τ_λ is either (1) geometrically transverse, or (2) one half of a simple clasp. By a regular homotopy that undoes each of the simple clasps, we can replace $(\mathbb{CP}^2, \mathcal{K})$ with an immersed surface $(\mathbb{CP}^2, \mathcal{L})$ that is geometrically transverse. In particular, each arc of each tangle $v_\lambda = \mathcal{L} \cap H_\lambda$ is transverse to the foliations by holomorphic disks. Furthermore, this regular homotopy does not change the bridge index.

Set $(Y, \xi) = (Y_1, \xi_1) \sqcup (Y_2, \xi_2) \sqcup (Y_3, \xi_3)$. Taking disjoint unions, we also obtain links $K = K_1 \sqcup K_2 \sqcup K_3$ and $L = L_1 \sqcup L_2 \sqcup L_3$ in Y , where L is transverse to ξ . For each simple clasp of τ_λ , choose a point $x \in H_\lambda$ in a tubular neighborhood of the Whitney disk. Let $\bar{x} \in -H_\lambda$ be its image in the mirror handlebody. Let \tilde{Y} be the 3-manifold obtained by surgery on the 0-sphere $\{x \cup \bar{x}\}$ for each simple clasp. Suppose there are n total clasps in τ . If both τ_α and τ_γ have clasps, then $\tilde{Y} \cong \#_{n-2} S^1 \times S^2$; if only τ_α has clasps, then $\tilde{Y} \cong \#_{n-1} S^1 \times S^2 \amalg S^3$. Each 0-sphere $\{x \cup \bar{x}\}$ is trivially isotropic in (Y, ξ) , thus we can perform contact surgery to obtain a contact 3-manifold $(\tilde{Y}, \tilde{\xi})$.

Lemma 6.1. *The contact structure $(\tilde{Y}, \tilde{\xi})$ is tight.*

Proof. Disjoint union preserves tightness, so (Y, ξ) is tight. Colin proved that contact 0-surgery preserves tightness [Col97], thus the resulting contact structure $(\tilde{Y}, \tilde{\xi})$ is tight. \square

Remark 6.2. The contact manifold $(\tilde{Y}, \tilde{\xi})$ has a 4-dimensional interpretation. Set

$$(\hat{Y}, \hat{\xi}) = (\hat{Y}_{1,N}, \hat{\xi}_{1,N}) \sqcup (\hat{Y}_{2,N}, \hat{\xi}_{1,N}) \sqcup (\hat{Y}_{3,N}, \hat{\xi}_{1,N}).$$

This is the boundary of a Stein domain $\hat{X}_N := \hat{X}_{1,N} \sqcup \hat{X}_{2,N} \sqcup \hat{X}_{3,N}$ whose complement in \mathbb{CP}^2 is a neighborhood of the spine of the trisection.

For each pair of points x, \bar{x} , we can choose a properly embedded arc in $\mathbb{CP}^2 \setminus \widehat{X}_N$ whose boundary are the corresponding points in $\widehat{Y}_{\lambda,N}$ and $\widehat{Y}_{\lambda-1,N}$. This arc is necessarily isotropic and therefore we can attach a Stein 1-handle to \widehat{X}_N whose core is this arc. For details, see [CE12]. After attaching all of the 1-handles, we obtain a Stein domain whose boundary is $(\widetilde{Y}, \widetilde{\xi})$.

Let \widetilde{K} be the link obtained from K by adding $2n$ untwisted, symmetric bands near the simple clasps as in Figure 14. Specifically, if two arcs τ_1, τ_2 form a simple clasp, we can find an untwisted, symmetric band connecting each pair $\tau_i, -\tau_i^r$ that runs across the 2-sphere created by surgery on $x \cup \bar{x}$. Resolving this band produces a new 4-component tangle. Repeating for all simple clasps yields the link \widetilde{K} . The same bands exist connecting v_1, v_2 to their mirrors. Let \widetilde{L} be the resulting link.

Proposition 6.3. *Let $\widetilde{K}, \widetilde{L}$ be the links obtained from K and L , respectively, by adding $2n$ bands.*

- (1) *The links \widetilde{K} and \widetilde{L} are isotopic.*
- (2) *The link \widetilde{K} bounds a ribbon surface F with*

$$\chi(F) = c_1 + c_2 + c_3 - 2n.$$

Proof. That the first statement is true near each simple clasp can be seen in Figure 14. Move all of the crossings of $\widetilde{\tau}$ in H_λ and then cancel by two Reidemeister II moves. Moreover, this local model occurs by assumption in a neighborhood of the Whitney disk, so we can simultaneously realize the isotopy at each simple clasp.

Secondly, the image of the link K in \widetilde{Y} is the unlink with $c_1 + c_2 + c_3$ components. Therefore it bounds a collection of disjoint, embedded disks. Then \widetilde{K} is obtained by surgering $2n$ bands to the unlink K and the surface F is the union of the original Seifert disks with these bands. \square

Proposition 6.4. *The link \widetilde{L} admits a transverse representative with self-linking number*

$$sl(\widetilde{L}) = d^2 - 3d - b + 2n.$$

Proof. The surface \mathcal{L} is geometrically transverse, so the link $L = L_1 \sqcup L_2 \sqcup L_3$ has self-linking number

$$sl(L) = d^2 - 3d - b$$

To prove the statement, we need to show that each band can be attached to L so that the result is transverse and so that each band increases the self-linking number by 1.

Topological 0-surgery on $x \cup \bar{x}$ is performed by cutting out B^3 neighborhoods of x and \bar{x} and then identifying their boundaries. To perform in the contact category, the boundaries must be convex surfaces with diffeomorphic characteristic foliations. For a thorough description, see [Gei08].

Take polar coordinates $(\theta_{\lambda+1}, r_\lambda, \theta_\lambda)$ on H_λ . Let $-H_\lambda$ denote H_λ with the orientation. Let $\Phi_\lambda : H_\lambda \rightarrow -H_\lambda$ be the identity map, which is an orientation-reversing diffeomorphism. We view H_λ as a subset of Y_λ and so it inherits the contact structure ξ_λ . A contact form defining the restriction of ξ_λ is

$$\alpha_+ = d\theta_{\lambda+1} + h_+(r)d\theta_\lambda$$

for some increasing function $h_+(r)$ satisfying $h_+(0) = 0$. In addition, we view $-H_\lambda$ as a subset of $Y_{\lambda-1}$ and it inherits the contact structure $\xi_{\lambda-1}$. Along the core $B_\lambda = \{r_\lambda = 0\}$ of the solid torus, the contact structure $\xi_{\lambda-1}$ is tangent to the foliation by holomorphic disks. Consequently, a contact form defining the restriction of $\xi_{\lambda-1}$ is

$$\alpha_- = -d\theta_{\lambda+1} + h_-(r)d\theta_\lambda$$

for some increasing function $h_-(r)$ satisfying $h_-(0) = 0$.

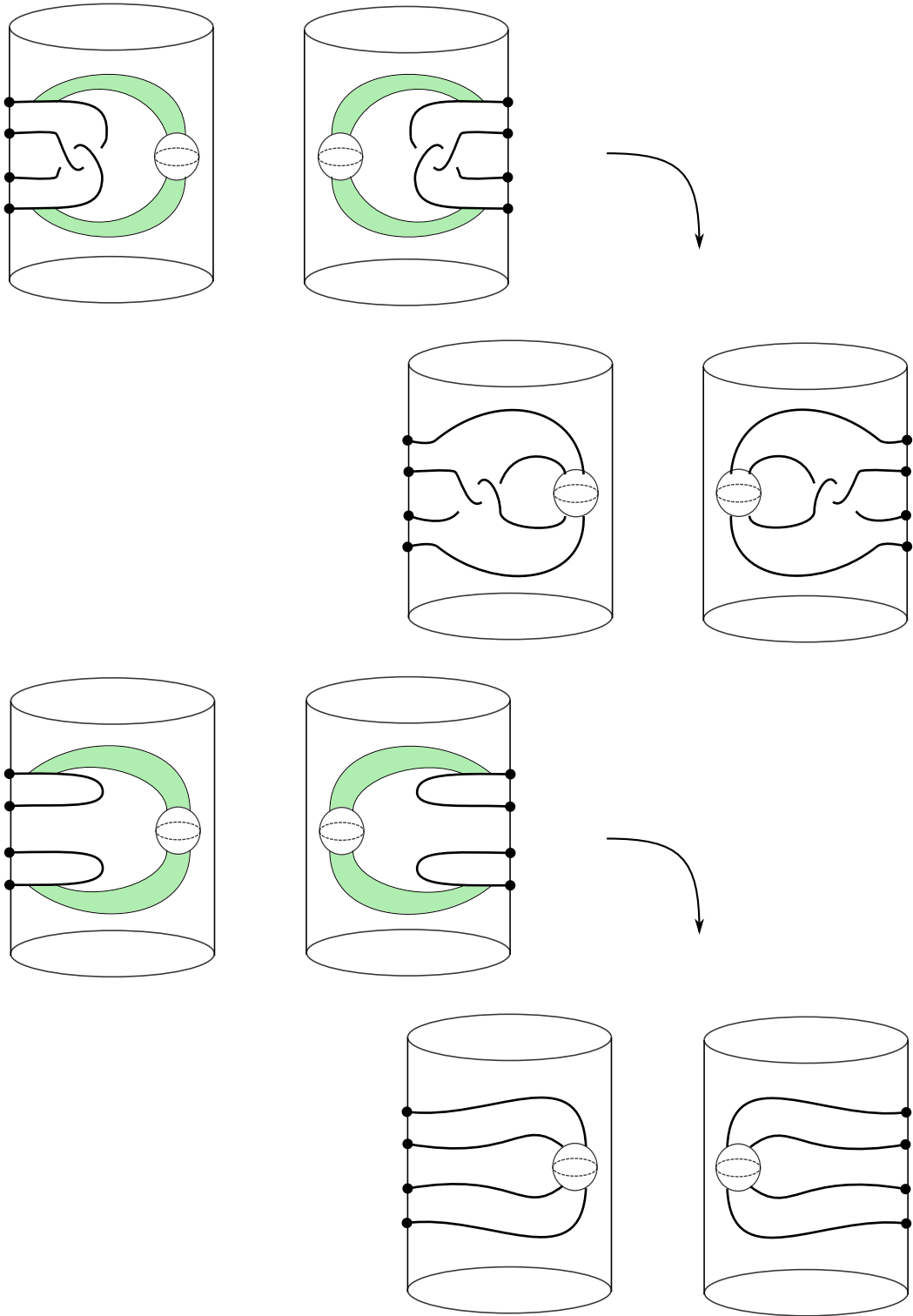


FIGURE 14. The effect of attaching symmetric bands in $H_\lambda \cup \overline{H}_\lambda$. (*Top Left*) Bands attached to $\tau \cup -\tau^r$. (*Middle Right*) The resulting tangle $\tilde{\tau}$. (*Middle Left*) Bands attached to $\nu \cup -\nu^r$. (*Bottom Right*) The resulting tangle $\tilde{\nu}$. The tangles $\tilde{\tau}$ and $\tilde{\nu}$ are isotopic.

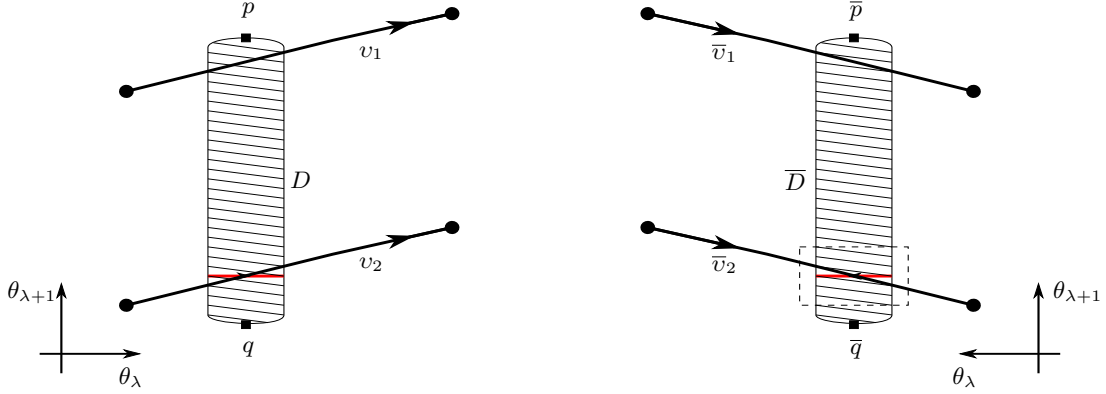


FIGURE 15. *Left:* The simple clasp τ_λ in H_λ . *Right:* The mirror τ_λ^r in $-H_\lambda$

By an isotopy, we can push each simple clasp into an arbitrary neighborhood of B_λ , where the contact structure is C^0 -close to the horizontal foliation. Choose a vertical disk D as in Figure 15 near the simple clasp, closer to the core of H_λ . And let $\bar{D} = \Phi_\lambda(D)$ be its mirror in $-H_\lambda$. The characteristic foliations on D and \bar{D} are illustrated in Figure 15 as well. Note that the contact structures are *not* mirrors.

Thicken D to a ball $\nu(D)$ with smooth boundary. We assume that the function $\theta_{\lambda+1}$, restricted to $\partial\nu(D)$, is Morse with a single maximum at p and single minimum at q . Let $\nu(\bar{D}), \bar{p}, \bar{q}$ denote mirrors in $-H_\lambda$. Near $\nu(D)$, the contact structure ξ_λ on H_λ is C^0 -close to the foliation $\ker(d\theta_{\lambda+1})$. Thus, we can assume that the contact structure has a positive tangency to $\nu(D)$ near p , a negative tangency near q and no other tangencies. This implies that the characteristic foliation \mathcal{F} of $\partial\nu(D)$ is the standard foliation on S^2 , consisting of trajectories connecting these two points. Similarly, near $\nu(\bar{D})$, the contact structure $\xi_{\lambda-1}$ on $-H_\lambda$ is C^0 -close to the foliation $-d\theta_{\lambda+1}$. Thus, we can assume that it has a positive tangency to $\nu(\bar{D})$ near \bar{q} , a negative tangency near \bar{p} and no other tangencies. Again, this determines the foliation $\bar{\mathcal{F}}$ of $\partial\nu(\bar{D})$.

The map Φ_λ restricts to an orientation-reversing diffeomorphism from $\partial\nu(D)$ to $\partial\nu(\bar{D})$. Thus we can use this identification to perform topological 0-surgery. However, since the contact structure $\xi_\lambda, \xi_{\lambda-1}$ are not mirrors, we need to replace Φ_λ by an isotopic map that identifies the characteristic foliations. Choose an arc $l = \{\theta_{\lambda+1} = \text{const}\}$ in D , oriented in the direction of θ_λ . Using the contact form α_+ described above, it is obvious that l is positively transverse to ξ_λ . Moreover, the mirror arc \bar{l} in $-H_\lambda$ is also positively transverse to $\xi_{\lambda-1}$. We can extend l and \bar{l} to simple closed curves on $\nu(D)$ and $\nu(\bar{D})$ that are everywhere transverse to the characteristic foliations. It is now clear there is an isotopy of Φ_λ to an orientation-reversing diffeomorphism that matches characteristic foliations

Now, via a transverse isotopy, we can flatten each arc v_i to agree with some arc l along the disk D and push it across $\partial\nu(D) \simeq \partial\nu(\bar{D})$ into $-H_\lambda$. It appears in $-H_\lambda$ as on the left of Figure 16. The symmetric band is also depicted in Figure 16 and attaching it is equivalent to resolving the negative crossing. The result is the righthand side of Figure 16. We can assume the resulting arcs of \bar{L} are transverse to the horizontal foliation, with is C^0 -close to $\xi_{\lambda-1}$, and therefore the resulting link can be assumed transverse. We can choose a local model where u_i, \bar{u}_i are two braid strands and attaching the band corresponds to adding a single positive crossing. A standard computation shows that the effect is to increase the self-linking number by 1.

Repeating for all n simple clasps, we obtain a transverse link L with the required self-linking number. \square

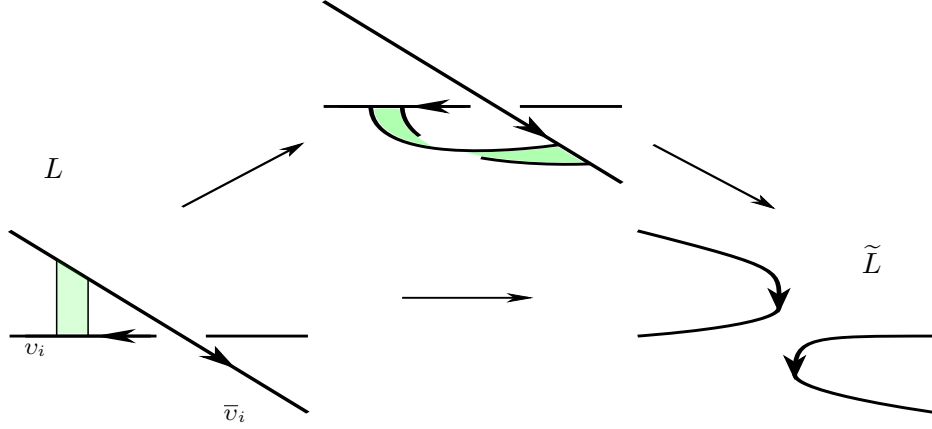


FIGURE 16. All figures represent the interior of the dotted box on the right side of Figure 15. *Left:* The symmetric band to attach to L . *Middle:* The band is isotopic to a band with a single positive twist. *Right:* Attaching the band is equivalent to resolving the crossing in the diagram, which can clearly be made transverse to the contact structure $\xi_{\lambda+1} = \ker(\alpha_-)$.

We can now prove the Thom conjecture.

Proof of Theorem 1.1. Let $(\mathbb{CP}^2, \mathcal{K})$ be an embedded, oriented, connected surface of degree $d > 0$. By Theorem 1.8 we can isotope \mathcal{K} into bridge position and by Proposition 4.4, we can assume that \mathcal{K} is in algebraically transverse bridge position. Furthermore, by Proposition 4.8, we can assume that the only obstruction to geometric transversality are n simple clasps. Combining Propositions 6.3 and 6.4, we can obtain a transverse link \tilde{L} that bounds a ribbon surface F with $\chi(F) = c_1 + c_2 + c_3 - 2n$ and such that

$$sl(\tilde{L}) = d^2 - 3d - b + 2n.$$

Applying the ribbon-Bennequin inequality (Theorem 5.3), we see that

$$d^2 - 3d - b + 2n = sl(\tilde{L}) \leq -\chi(F) = -c_1 - c_2 - c_3 + 2n$$

Equivalently, we have that

$$\chi(\mathcal{K}) = c_1 + c_2 + c_3 - b \leq 3d - d^2$$

Solving for the genus, we have

$$g(\mathcal{K}) \geq \frac{1}{2}(d-1)(d-2)$$

\square

REFERENCES

- [Ben83] Daniel Bennequin. Entrelacements et équations de Pfaff. In *Third Schnepfenried geometry conference, Vol. 1 (Schnepfenried, 1982)*, volume 107 of *Astérisque*, pages 87–161. Soc. Math. France, Paris, 1983.
- [CE12] Kai Cieliebak and Yakov Eliashberg. *From Stein to Weinstein and back*, volume 59 of *American Mathematical Society Colloquium Publications*. American Mathematical Society, Providence, RI, 2012. Symplectic geometry of affine complex manifolds.
- [Col97] Vincent Colin. Chirurgies d’indice un et isotopies de sphères dans les variétés de contact tendues. *C. R. Acad. Sci. Paris Sér. I Math.*, 324(6):659–663, 1997.
- [Dym04] K. Dymara. Legendrian knots in overtwisted contact structures. *ArXiv Mathematics e-prints*, October 2004.
- [Eli92] Yakov Eliashberg. Contact 3-manifolds twenty years since J. Martinet’s work. *Ann. Inst. Fourier (Grenoble)*, 42(1-2):165–192, 1992.
- [Fc03] Franc Forstnerič. Stein domains in complex surfaces. *J. Geom. Anal.*, 13(1):77–94, 2003.
- [Fc17] Franc Forstnerič. *Stein manifolds and holomorphic mappings*, volume 56 of *Ergebnisse der Mathematik und ihrer Grenzgebiete. 3. Folge. A Series of Modern Surveys in Mathematics [Results in Mathematics and Related Areas. 3rd Series. A Series of Modern Surveys in Mathematics]*. Springer, Cham, second edition, 2017. The homotopy principle in complex analysis.
- [FS95] Ronald Fintushel and Ronald J. Stern. Immersed spheres in 4-manifolds and the immersed Thom conjecture. *Turkish J. Math.*, 19(2):145–157, 1995.
- [Gei08] Hansjörg Geiges. *An introduction to contact topology*, volume 109 of *Cambridge Studies in Advanced Mathematics*. Cambridge University Press, Cambridge, 2008.
- [GK16] David Gay and Robion Kirby. Trisecting 4-manifolds. *Geom. Topol.*, 20(6):3097–3132, 2016.
- [KM93] P. B. Kronheimer and T. S. Mrowka. Gauge theory for embedded surfaces. I. *Topology*, 32(4):773–826, 1993.
- [KM94] P. B. Kronheimer and T. S. Mrowka. The genus of embedded surfaces in the projective plane. *Math. Res. Lett.*, 1(6):797–808, 1994.
- [KM95] P. B. Kronheimer and T. S. Mrowka. Embedded surfaces and the structure of Donaldson’s polynomial invariants. *J. Differential Geom.*, 41(3):573–734, 1995.
- [KP11] Keiko Kawamuro and Elena Pavelescu. The self-linking number in annulus and pants open book decompositions. *Algebr. Geom. Topol.*, 11(1):553–585, 2011.
- [Law97] Terry Lawson. The minimal genus problem. *Exposition. Math.*, 15(5):385–431, 1997.
- [LM98] P. Lisca and G. Matić. Stein 4-manifolds with boundary and contact structures. *Topology Appl.*, 88(1-2):55–66, 1998. Symplectic, contact and low-dimensional topology (Athens, GA, 1996).
- [LM18] Peter Lambert-Cole and Jeffrey Meier. Bridge trisections in rational surfaces. 2018.
- [MST96] John W. Morgan, Zoltán Szabó, and Clifford Henry Taubes. A product formula for the Seiberg-Witten invariants and the generalized Thom conjecture. *J. Differential Geom.*, 44(4):706–788, 1996.
- [MZ17a] J. Meier and A. Zupan. Bridge trisections of knotted surfaces in 4-manifolds. *ArXiv e-prints*, October 2017.
- [MZ17b] Jeffrey Meier and Alexander Zupan. Bridge trisections of knotted surfaces in S^4 . *Trans. Amer. Math. Soc.*, 369(10):7343–7386, 2017.
- [OS00a] Peter Ozsváth and Zoltán Szabó. Higher type adjunction inequalities in Seiberg-Witten theory. *J. Differential Geom.*, 55(3):385–440, 2000.
- [OS00b] Peter Ozsváth and Zoltán Szabó. The symplectic Thom conjecture. *Ann. of Math. (2)*, 151(1):93–124, 2000.
- [OS03] Peter Ozsváth and Zoltán Szabó. Absolutely graded Floer homologies and intersection forms for four-manifolds with boundary. *Adv. Math.*, 173(2):179–261, 2003.
- [OS04] Peter Ozsváth and Zoltán Szabó. Holomorphic triangle invariants and the topology of symplectic four-manifolds. *Duke Math. J.*, 121(1):1–34, 2004.
- [Ras10] Jacob Rasmussen. Khovanov homology and the slice genus. *Invent. Math.*, 182(2):419–447, 2010.
- [Rud93] Lee Rudolph. Quasipositivity as an obstruction to sliceness. *Bull. Amer. Math. Soc. (N.S.)*, 29(1):51–59, 1993.
- [Sar11] Sucharit Sarkar. Grid diagrams and the Ozsváth-Szabó tau-invariant. *Math. Res. Lett.*, 18(6):1239–1257, 2011.
- [Shu07] Alexander N. Shumakovitch. Rasmussen invariant, slice-Bennequin inequality, and sliceness of knots. *J. Knot Theory Ramifications*, 16(10):1403–1412, 2007.
- [Str03] Søren Strle. Bounds on genus and geometric intersections from cylindrical end moduli spaces. *J. Differential Geom.*, 65(3):469–511, 2003.

SCHOOL OF MATHEMATICS, GEORGIA INSTITUTE OF TECHNOLOGY

E-mail address: `plc@math.gatech.edu`

URL: <http://www.math.gatech.edu/~plambertcole3>